NAVAL POSTGRADUATE SCHOOL

MONTEREY, CALIFORNIA

THESIS

STALL PRECURSOR DETERMINATION OF AN LM-2500 GAS TURBINE

by

Gustave C. Dahl

June 2007

Thesis Advisor:	Knox Millsaps
Second Reader:	Garth Hobson

THIS PAGE INTENTIONALLY LEFT BLANK

REPORT DOCUMENTATION PAGE			Form Approved OMB No. 0704-0188
Public reporting burden for this collection of information is estimated to average 1 hour per response, including the time for reviewing instruction, searching existing data sources, gathering and maintaining the data needed, and completing and reviewing the collection of information. Send comments regarding this burden estimate or any other aspect of this collection of information, including suggestions for reducing this burden, to Washington headquarters Services, Directorate for Information Operations and Reports, 1215 Jefferson Davis Highway, Suite 1204, Arlington, VA 22202-4302, and to the Office of Management and Budget, Paperwork Reduction Project (0704-0188) Washington DC 20503.			
1. AGENCY USE ONLY ***(Leave blank)***	**2. REPORT DATE** June 2007	**3. REPORT TYPE AND DATES COVERED** Master's Thesis	
4. TITLE AND SUBTITLE: Stall Precursor Determination of an LM-2500 Gas Turbine		**5. FUNDING NUMBERS**	
6. AUTHOR(S) Gustave C. Dahl			
7. PERFORMING ORGANIZATION NAME(S) AND ADDRESS(ES) Naval Postgraduate School Monterey, CA 93943-5000		**8. PERFORMING ORGANIZATION REPORT NUMBER**	
9. SPONSORING /MONITORING AGENCY NAME(S) AND ADDRESS(ES) N/A		**10. SPONSORING/MONITORING AGENCY REPORT NUMBER**	
11. SUPPLEMENTARY NOTES The views expressed in this thesis are those of the author and do not reflect the official policy or position of the Department of Defense or the U.S. Government.			
12a. DISTRIBUTION / AVAILABILITY STATEMENT Approved for public release; distribution is unlimited		**12b. DISTRIBUTION CODE**	

13. ABSTRACT (maximum 200 words)

This thesis presents an analysis of data taken from several stall initiation events for an LM-2500 gas turbine engine. Specifically, the time series of three separate pressure signals located at stages 3, 6, and 15 were analyzed utilizing fast Fourier transform, power spectral density, and an autocorrelation technique to determine the best and most reliable indicator to stall. The spectral analyses performed showed that rotating precursor waves that travel at approximately half rotor speed were the best indicators. Several algorithms were used and it was determined that stall wave perturbations can be identified reliable about 880 revolutions prior to the stall. This work indicates that a single pressure signal located at stage 3 on an LM-2500 gas turbine can be used to give advance warning to a stall more than 2 seconds prior to the stall event.

14. SUBJECT TERMS Stall Precursor, Stall Detection, Compressor Stall, Stall Wave Perturbation, Gas Turbine, Fast Fourier Transform, FFT, Power Spectral Density, PSD, Autocorrelation			**15. NUMBER OF PAGES** 85
			16. PRICE CODE
17. SECURITY CLASSIFICATION OF REPORT Unclassified	**18. SECURITY CLASSIFICATION OF THIS PAGE** Unclassified	**19. SECURITY CLASSIFICATION OF ABSTRACT** Unclassified	**20. LIMITATION OF ABSTRACT** UL

NSN 7540-01-280-5500

Standard Form 298 (Rev. 2-89)
Prescribed by ANSI Std. 239-18

THIS PAGE INTENTIONALLY LEFT BLANK

Approved for public release; distribution is unlimited

STALL PRECURSOR DETERMINATION OF AN LM-2500 GAS TURBINE

Gustave C. Dahl
Lieutenant, United States Navy
B.S., Milwaukee School of Engineering, 2000

Submitted in partial fulfillment of the
requirements for the degree of

MASTER OF SCIENCE IN MECHANICAL ENGINEERING

from the

NAVAL POSTGRADUATE SCHOOL
June 2007

Author: Gustave C. Dahl

Approved by: Knox T. Millsaps
Thesis Advisor

Garth V. Hobson
Second Reader

Anthony J. Healey
Chairman, Department of Mechanical and Astronautical Engineering

THIS PAGE INTENTIONALLY LEFT BLANK

ABSTRACT

This thesis presents an analysis of data taken from several stall initiation events for an LM-2500 gas turbine engine. Specifically, the time series of three separate pressure signals located at stages 3, 6, and 15 were analyzed utilizing fast Fourier transform, power spectral density, and an autocorrelation technique to determine the best and most reliable indicator to stall. The spectral analyses performed showed that rotating precursor waves that travel at approximately half rotor speed were the best indicators. Several algorithms were used and it was determined that stall wave perturbations can be identified reliable about 880 revolutions prior to the stall. This work indicates that a single pressure signal located at stage 3 on an LM-2500 gas turbine can be used to give advance warning to a stall more than 2 seconds prior to the stall event.

THIS PAGE INTENTIONALLY LEFT BLANK

TABLE OF CONTENTS

LIST OF FIGURES

LIST OF TABLES

THIS PAGE INTENTIONALLY LEFT BLANK

ACKNOWLEDGMENTS

The author would like to thank Professor Knox Millsaps for his help throughout this project. His insight with digital signal processing and gas turbine dynamics was instrumental in completing this project. Professor Garth Hobson is also thanked for his willingness to share knowledge on stall wave perturbations, and for being the second reader.

THIS PAGE INTENTIONALLY LEFT BLANK

I. INTRODUCTION

A. OVERVIEW

The General Electric LM-2500 gas turbine engine is used in a large portion of the United States Navy's marine applications as main propulsion prime movers. The Navy depends on the LM-2500 gas turbine engine to provide power throughout the fleet.

The LM-2500, as well as other compressors, is susceptible to instabilities. The specific instabilities of concern are rotating stalls and surge. These stall instabilities not only can cause engine damage, but they can also reduce the overall operability of the gas turbine. It is in the interest of General Electric and the United States Navy to be able to predict when stall is about to occur. Effective stall prediction would reduce the possibility of damage to the compressor.

Rotating stall and surge instabilities occur when a compressor is operating above the compressors surge line as depicted on the LM-2500 compressor map below.

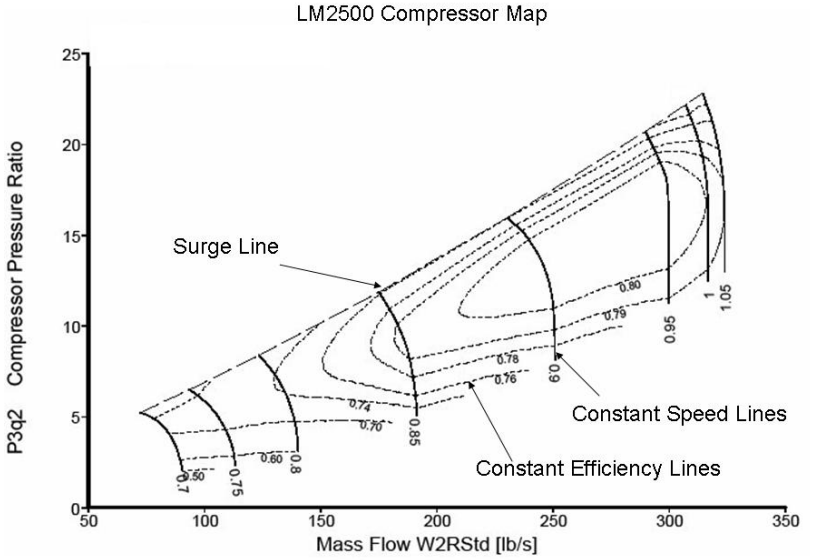

Figure 1. LM2500 Compressor Map

In order to reduce the possibility of stall, compressors and turbines are matched so that the nominal steady state operating lines are well away from the compressor's surge line.

The engine response may be limited due to a reduced operating envelope imposed to prevent operating near the compressor's surge line. If a rapid increase in output is needed the operator is limited due to this operating envelope and therefore cannot provide the desired response in an emergency situation. If an operator or computer feedback system were able to predict oncoming stall instabilities and thus prevent it from occurring the operating region could be expanded. This expansion would allow the operator to take full advantage of the compressor and minimize the shortcomings involved in a reduced envelope.

There has been a tremendous amount of work done over the years in an attempt to predict stall instabilities within gas turbine engines. Many different types of compressors have been analyzed utilizing a variety of digital signal processing techniques to determine if a stall precursor could be detected. There currently is no method of stall prediction utilized on the LM-2500 gas turbine engine.

A short summary of previous work will be presented to understand the types of processing techniques that have been used. This review will also be used to determine the best location to find stall precursors. The emphasis will be placed on the history of stall precursor detection methods. Each article will be summarized to determine the methods used and to annotate significant findings from their work. The final section of this chapter will state the objectives for this thesis work that will involve data obtained for the LM-2500 compressor.

B. LITERATURE REVIEW

Emmons et al. (1955)

Compressor instabilities were researched by Emmons et al. [1] in 1955. This work was one of, if not the first, to distinguish between rotating and surge stalls. They studied both centrifugal and axial compressors and noted distinct differences in rotating and surge stalls. They described a surge stall as a Helmholtz resonance in the machine, and the rotating stall as the propagation of stall from blade to blade in the machine. They also noted that the shape, size and number of cells could vary by the type of compressor or the operating condition. Although this work did not provide any models for stall, it did establish a baseline for future research into compressor stalls and led to discussions of pre-stall behavior.

N. M. McDougall, N. A. Cumpsty, and T. P. Hynes (1990)

In 1990, McDougall et al. [2] performed detailed measurements on an axial compressor in order to look at the fluid mechanics of the flow during stall. They were able to show that low order perturbations existed in the flow rates prior to each of the stall events. Their findings indicated that a low order mode is dominant prior to stall and that it can be observed with hot wires well before the actual stall takes place. McDougall et al., concluded in their work that through a Fourier analysis, they could predict these low order modes in advance of a stall occurrence. These low order modes were shown to rise and fall in amplitude well prior to the stall and only grew to a significant value close to the stall event. They noted that a controller would need to have a significant amplitude change in the flow rates in order to accurately detect the stall precursor, and that the significant amplitude growth of low order magnitude waves could be used in this fashion.

M. Inoue, M. Kuroumaru, T. Iwamoto, and Y. Ando (1991)

A subsequent argument was made in 1991 by Inoue et al. [3] showing that stall precursors could be determined by monitoring the collapse of the periodicity in pressure fluctuations using a single pressure sensor. They utilized a pseudo-

spatial correlation technique to determine the breakdown in periodicity and determined that a rotating stall precursor could be detected in this manner. Although this was done on rotors with small blade numbers (12 to 16), it may prove to be a useful technique on rotors with more blades or machines with different geometrical properties.

I. J. Day (1993)

Day [4] performed a follow on test on axial flow compressors on both single stage and multi stage machines. He wanted to determine the wave development prior to stall in order to have a better understanding of the process. His analysis determined that the modal oscillations that were previously noted by McDougall et al. were actually separate events from the formation of stall cells. They also found that these two events do not necessarily have to happen consecutively and that either one may be the first to appear. The stall cell can form before the modal oscillations and or the modal oscillations before the stall cell.

They found that the stall cell formation could be classified into two separate categories. These categories are small time scale events or large time scale events. The distinction between the two is one of speed at which they rotate and not the size of the cell when it forms. He found a variety of instances in which these can occur but concluded that given their data the more likely event was of a short time length scale disturbance resulting in the subsequent stall.

M. Tryfonidis, O. Etchevers, J. D. Paduano, A. H. Epstein, and G. J. Hendricks (1995)

Nine separate compressors were analyzed for stall precursors in 1995 by Tryfonidis et al. [5] in order to compare their results to previous stability work. Their work resulted in the “Traveling Wave Energy” method that looked at the energy of the waves as they traveled through time. In every one of the compressors analyzed it was determined that small amplitude pre-stall traveling waves were present before the stall event. The traveling wave structure was dependent on the corrected speed of the machine. It showed that a wave

rotating at ½ the shaft frequency will grow strongly at low speeds while a shaft frequency disturbance dominates at 100 percent speed. If the machine is at a constant speed the structure is a function of the position on the compressor speed-line. They noted in their analysis that stall precedes surge in every instance. Through the use of this traveling wave energy they were able to consistently have 100-200 revolutions of warning prior to the stall event.

M. M. Bright, H. K. Qammar, H. J. Weigl, and J. D. Paduano (1997)

Bright et al. [6] in 1997 proposed to use a chaotic time series analysis method, specifically a correlation method to give advance warning of stall events. The improvement over the traveling wave energy method as proposed by Tryfonidis et al. is that the correlation method only requires one sensor for detection. Bright et al. used a comparison between their method and the traveling wave energy method to determine the validity of their findings.

The results indicated that with the correlation method could predict stall even before the traveling wave energy method. The research proved the correlation method will work; however, it was all done in a post processing environment due to the computational complexity of the method. It was determined that further research would need to be done to implement the method in a real time application.

T. R. Camp, and I. J. Day (1998)

Camp et al. [7] tried to obtain a better understanding of previous work done by Day in 1993. They researched the differences in the short and long time scale events that occur prior to a stall. This further investigation showed that modes and spikes can both occur at the same time in the same compressor. They showed that long length scale disturbances were related to a two dimensional instability of the whole compressor system where as the short length scale disturbances indicated a three dimensional breakdown of the flow field due to high rotor incidence angles. They also showed that each type of disturbance can be influenced in high speed compressors by changing the shaft speed of the machine.

D. A. Hoying (1995)

Hoying [8] performed a study on a high speed axial compressor utilizing pressure sensors around the annulus of the compressor. These data were analyzed using spatial Fourier Transforms to determine the existence and stability of pre-stall waves.

This research found that the waves existed prior to stall in all cases, and that the length of time before a stall was dependent on the compressor speed. He found that the waves were present for more revolutions before low speed stalls and were present for fewer revolutions at higher speed stalls.

I. J. Day, T. Breuer, J. Escuret, M. Cherrett, and A. Wilson (1999)

Day et al. [9] looked extensively at the prospects for active control in four different high speed compressors over a full range of speed. This research delineated even more differences between modal oscillations (long length scale disturbances) and spikes (short length scale disturbances) as noted in previous work performed by Day. In their work they instrumented each of the machines both axially and circumferentially in order to obtain a complete picture of the activity in the machine.

In order to validate previous work, they noted that both modal and spike disturbances existed in all four machines. They also noted that modal type disturbances are the easiest to detect because they affect the whole machine; therefore, all probes that were placed on the machine detected the event. On the other hand the spike disturbances that were found in low speed operations are harder to detect because only one probe at a time will notice the disturbance.

They found that there are a variety of other variables that could have an influence in the active control of a compressor. These include front end start up stall, high frequency stall, abrupt stalling at full speed, fix location stall, shaft order disturbances, and distorted inlet flow. Each of these may not affect every compressor, but the possibilities of other types of stalls to occur have to be addressed in any type of active stall control system.

M. M. Bright, H. K. Qammar, and L. Wang (1999)

Bright et al. [10] further investigated previous work on the correlation method in pre-stall detection analysis. The correlation method was able to detect both short and long length scale disturbances in compressors, but it was noted that due to computational complexity this method is best suited for a post processing application. In order to achieve real time application another method would be better suited to this task.

B. Hoss, D. Leinhos, and L. Fottner (2000)

Hoss et al. [11] investigated pre-stall behavior on a two spool turbofan engine. They used Fourier, power spectral density, and wavelet techniques to determine the applicability of each to their specific engine. The methods they used included time domain, Fourier frequency domain, power spectral density and wavelet analysis.

They found the existence of short and long length scale disturbances but also showed that forcing functions in a particular engine installation play an important role in any analysis. Their findings state that the controlling unit will have to detect oscillatory events as well as control both external and internal forcing functions.

C. SUMMARY

The previous work has provided a good understanding of how a variety of engines were tested and then data analyzed with Fourier analysis, Power Spectral Density, along with correlation methods to determine if stall precursors existed. The literature review was able to highlight that although each engine will have different pre-stall characteristics they do show modal oscillations at approximately one half of rotor speed. What is not known is if these same analyses will show modal oscillations in an LM-2500 engine that is brought to stall.

D. OBJECTIVES

In light of this review and the techniques used, the following objectives have been set:

- Perform a Fourier analysis with the available data on the LM-2500 and determine if stall wave perturbations exist.
- With this Fourier analysis, determine the Power Spectral Density of the frequency spectrum. Utilize the change in Power Spectral Density to conclude if this technique can be used to detect stall waves.
- Perform a correlation analysis on the available data to determine if stall precursors can be detected utilizing correlation techniques.
- Determine the frequencies in the engine where stall precursors exist and recommend the best available sensor along with the best analytical technique to be used.

II. EXPERIMENTAL SETUP

A. EXPERIMENT OVERVIEW

A series of tests were performed on June 27 and June 28, 2005 on an LM-2500 Gas Turbine to verify a General Electric stall detection algorithm. This test was performed at the Land Based Engineering Site (LBES) at Naval Sea Systems Command in Philadelphia, PA. During this test a series of data were taken for future analysis to include the pressure signals from three separate locations. The engine was brought closer to the surge line by varying the variable stator vanes. In order for the variable stator vanes to be varied the control system was altered to allow for an artificial input.

There were four separate data runs that produced engine stoppage. Each one was conducted at a different gas generator speed. The data that were captured will be analyzed to complete the objectives of this research. This chapter provides a description of the known information about each of these data runs.

B. AVAILABLE SENSORS

The data included for analysis consisted of seven tracks. Seven sensors are listed corresponding to the tracks in the table below:

Track	Sensor
1	Pressure Sensor
2	Pressure Sensor
3	Pressure Sensor
4	Raw Vibration Sensor
5	Light-Off Detector
6	Silicon Carbide Gas Sensor
7	Raw Vibration Sensor

Table 1. Available Sensors

The sensors used for this research were from the three pressure sensors located at three separate stages in the engine. These three sensors were mounted in borescope ports on the engine. The first pressure sensor was located in stage 3 of the compressor, the second was mounted in stage 6, and the third was mounted in stage 15. In each case the pressure sensors location is aft of the stage in the compressor.

The location of the three pressure sensors is depicted in the figure below.

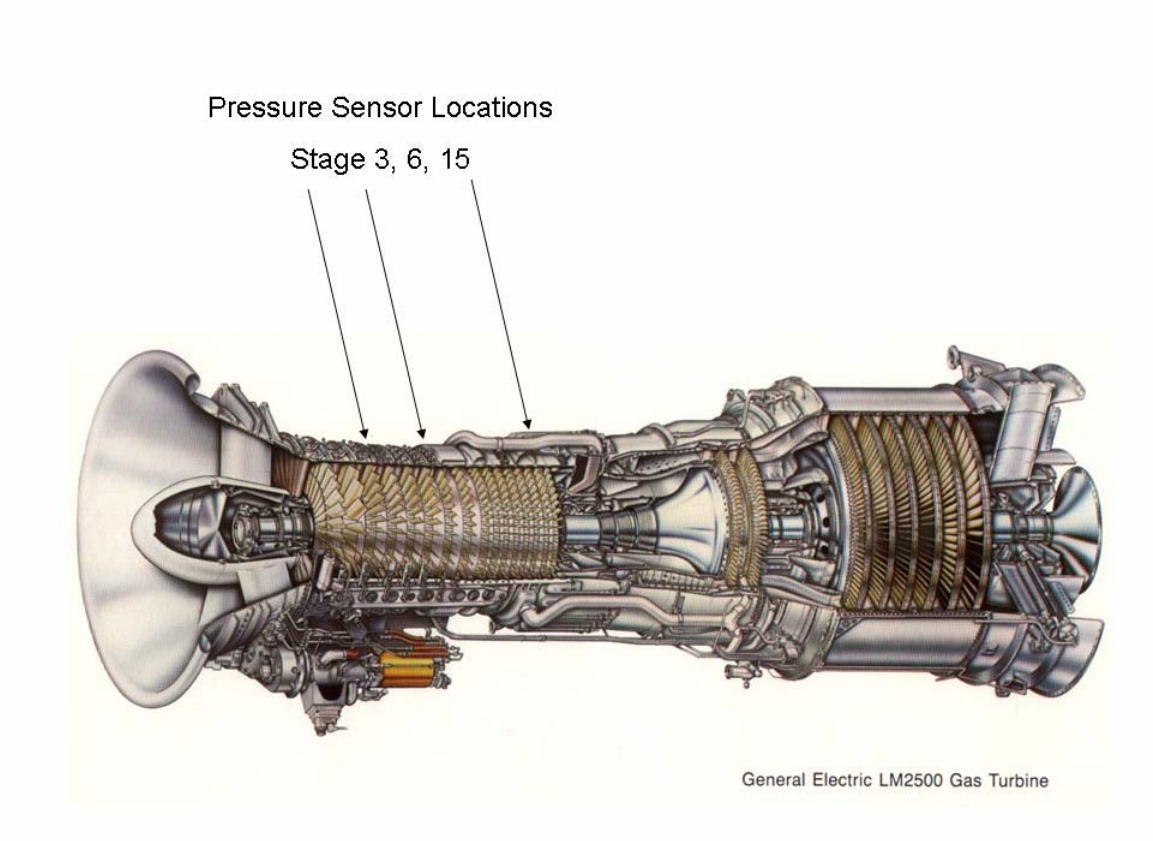

Figure 2. Pressure Sensor Locations

C. DATA RUNS

1. Flameout Trip Description

On June 27, 2005, a stall test was attempted at low speed. The gas generator was operating at 7,000 RPM and the power turbine was operating at 1335 RPM. The operators began vane motion at 15:25. At 15:31 the vanes were 28 degrees to the open. The engine tripped at 15:40 with the variable stator vanes at 31 degrees to the open.

The operators noted that they did not hear any loud bangs in the control room during this test. The data provided includes 116 seconds of data from seven sensors in total.

A summary of the known information is found in the following table.

GG Speed (RPM)	7000	
PT Speed (RPM)	1335	
Data Length (Seconds)	116	
Time	Vane (Degrees)	Test Time
15:25	Unknown	Start
15:31	28	
15:40	31	Stop

Table 2. Flameout Trip Data Summary

2. High Vibration Trip Description

On June 27, 2005 an additional stall test was attempted at low speed. The gas generator was operating at 7,500 RPM. The operators increased the power turbine speed from 1,805 RPM at 16:15 to 2,050 RPM at 16:18 during this test. The variable stator vane locations and times are unknown for this test run.

The operators noted that they did not hear any loud bangs in the control room during this test. The data provided includes 95 seconds of data from seven sensors.

A summary of the known information is found in the following table.

GG Speed (RPM)	7500	
PT Speed (RPM)	1805 - 2050	
Data Length (Seconds)	95	
Time	PT Speed (RPM)	Test Time
16:15	1805	
16:16	2000	
16:18	2050	
16:18	Unknown	Stop

Table 3. High Vibration Data Summary

3. Engine Trip Description

On June 28, 2005 a stall test was attempted at low speed. The gas generator and power turbine speeds are unknown for this data run. The variable stator vane locations and times are also unknown.

The operators noted that they did not hear any loud noises in the control room. The data provided includes 162 seconds from seven sensors.

A summary of the known information is found in the following table.

GG Speed (RPM)	Unknown
PT Speed (RPM)	Unknown
Data Length (Seconds)	162
Time	Test Time
Unknown	Start
Unknown	Stop

Table 4. Engine Trip Data Summary

4. High-Speed Stall Test Description

The final engine run was recorded on June 28, 2005. This test was a high-speed stall test with the gas generator running at 8,800 RPM. The power turbine was 2,800 RPM for this test. Vane motion began at 15:44 with the final vane location at 5 degrees to the open at engine stoppage.

The operators heard four loud bangs in the control room during this test. They believed that this was the most significant test performed. The data that was provided includes the full record of information in 20-second intervals.

A summary of the known information about this data run is found in the following table.

GG Speed (RPM)	8800	
PT Speed (RPM)	2800	
Data Length (Seconds)	Full	
Time	Vane (Degrees)	Test Time
15:44	Unknown	Start
15:45	2	
15:46	3	
15:48	5	Stop

Table 5. High-Speed Stall Data Summary

D. ADDITIONAL INFORMATION

There is some additional information that was available to assist with data analysis. The sampling frequency for the three pressure sensors were performed at 51.2 kHz. There was instrument noise present at 60 Hz at about 4-5 mV RMS on all channels of data that was provided. The available speed information from an additional sensor did not work and is unusable for these data sets.

The high-speed stall test run will be the primary data set analyzed for this research due to the operators hearing indication of an actual stall occurring. The remaining three data runs will be analyzed after digital signal processing techniques are established utilizing the high-speed run.

THIS PAGE INTENTIONALLY LEFT BLANK

III. SIGNAL PROCESSING TECHNIQUES

A. OVERVIEW

There are a variety of ways to utilize digital signal processing to analyze time series data. The most utilized method, and what has been used extensively in previous work, is the Fourier Transform. Performing a Fourier analysis on the data can be used to determine the frequencies and phases of the harmonic components. The Fourier analysis results can then be used to determine the Power Spectral Density of the spectrum. The Power Spectral Density takes the real and imaginary components of a Fourier analysis and provides an estimation of the energy in the signal. The other technique that will be implemented is the autocorrelation technique. Autocorrelation is performed to correlate a data series with itself. This chapter will discuss the theory behind each digital processing technique.

B. TIME SERIES

The data that will be analyzed are provided in a pressure versus time format. The first analysis technique is a plot of pressure versus time. These plots can be used to determine the approximate time of engine stoppage due to the large pressure fluctuations that develop.

C. FOURIER TRANSFORMS

The primary purpose of a Fourier transform is to obtain the spectral information from a data series. In order to analyze information from any data series a discrete Fourier transform must be used in the following form [12]:

$$X_n(e^{j\omega_k}) = \sum_{n=0}^{N-1} x(n) e^{\frac{-j2\pi kn}{N}} \tag{1}$$

The above equation is valid for k = 0,1,…,N-1, with N2 complex multiplications and additions required to perform the transform.

In order to reduce the required calculations and increase the efficiency, Fourier transform algorithms have been developed to produce the fast Fourier transform (FFT). The FFT algorithms reduce the number of required calculations from N2 to NlogN multiplications and additions. The reduction in calculation time can be significant enough to allow application of Fourier transforms where they otherwise could not be used.

In order to utilize the increased efficiency of these FFT algorithms on the given data a software program called Matlab has been used. Matlab has built in FFT functions that utilize Cooley-Turkey [13] based algorithms. The FFT is implemented utilizing the following Matlab function:

$$Y = fft(X, N) \tag{2}$$

Where X is the vector of the associated data points to be analyzed and N is the length of the FFT desired. If N is greater than the length of the vector X, the vector is then padded with zeros to obtain the desired length. If the vector X is less than the desired FFT length, it is truncated to accommodate the desired size. The FFT computation is the fastest when N is a power of two. The analyses performed in this research all have FFT lengths as a factor of two.

The resulting FFT from this algorithm in and of itself will not produce the results that are required to effectively analyze the data, because the FFT vector produced contains a mirror image of the resulting frequency spectrum. The FFT needs to be reduced in order to eliminate this symmetry. Since the FFT vector length is known due to it being an input to the FFT function the second half of the vector is eliminated.

D. POWER SPECTRAL DENSITY (PSD)

The FFT analyses performed utilizing Matlab provides for the opportunity to determine the PSD of the spectrum as a function of frequency. The FFT analysis performed above results in a vector that contains real and imaginary parts.

With the FFT above we can compute the Power Spectral Density (PSD) of this spectrum by taking the values of the FFT and multiplying it by its complex conjugate. This results in an estimation of the energy at all frequencies in the spectrum.

E. CORRELATION

Correlation is a statistical tool that can be used on a time series to determine how well that series correlates with another series. When a data series is correlated with itself it is called autocorrelation. In this research autocorrelation was used to determine the extent of correlation. The data were correlated with itself at a specified lag. Autocorrelation [12] is defined as:

$$r_{xx}(n_1, n_2) = E\{x(n_1)\overline{x}(n_2)\} \quad (3)$$

Where $x(n_1)$ and $x(n_2)$ are associated with the same time series at a time lag apart.

THIS PAGE INTENTIONALLY LEFT BLANK

IV. RESULTS

A. OVERVIEW

This chapter will show the results of the signal processing techniques detailed in the previous chapter. These signal processing techniques were performed and analyzed on each of the data runs. It is necessary to start the analysis with the high-speed stall engine run due to the operators having audible indication of the stall. The results of the high-speed run are then used on the remaining three data runs to determine if a characteristic stall event was the cause for that particular engine stoppage. This chapter will also determine which of the pressure sensors should be used to detect stall precursors as well as the best signal processing technique.

B. HIGH-SPEED STALL

The high-speed stall run was performed at a constant gas generator speed of 8,800 RPM with a slow opening of the vanes to five degrees open when the engine tripped. The stall was audibly detected by the four loud bangs heard in the control room. The provided data were divided into 20-second intervals for easier manipulation, and by looking at the data and pressure variations it was determined that the stall event occurred in the sixteenth segment of the given data. The sampling frequency for the provided pressure sensors was 51.2 kHz. The data will be looked at first with a pressure versus time plot, and the remainder of this section devoted to the other digital signal processing techniques.

1. Time Series

The sixteenth segment of data was first plotted for the three pressure signals on a pressure versus time plot to determine the exact time of stall and to analyze the pressure changes occurring in the engine. The figure below shows the three pressure plots around the time of the engine stoppage. The plots were reduced to a two second interval when the engine stopped. The stages monitored are stage 3, 6, and 15.

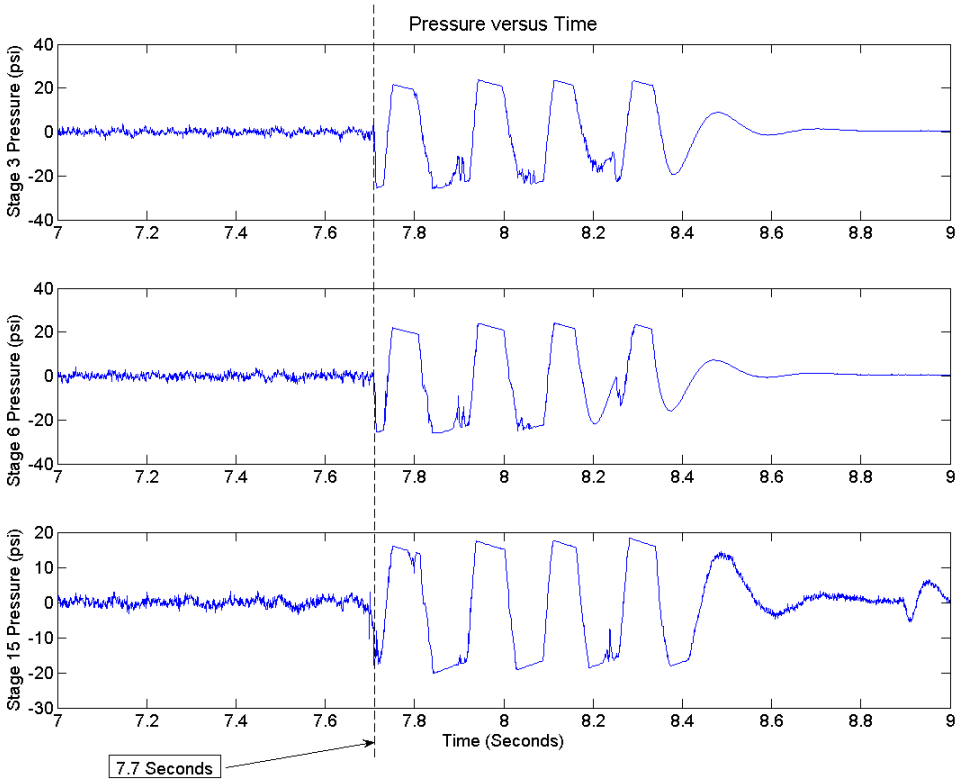

Figure 3. High-Speed Stall Pressure versus Time

The above figure shows the four loud bangs that were heard in the control room during the engine run. This is the sixteenth segment of the provided data series and it indicates that the engine stopped at approximately 7.7 seconds into this 20-second segment. The exact stall time is not known through the given information; however, the above plot allows for a good estimation of the appropriate time.

2. FFT and PSD Analysis

The gas turbine for this data run was running at 8,800 RPM or 146.6 Hz. The figure below was run with a FFT size of 32,768 in order to provide the detail required to see frequencies as low as 60 Hz with a sampling frequency of 51.2 kHz. The data analyzed consists of a 40-second sample in order to capture an adequate history before the engine stopped.

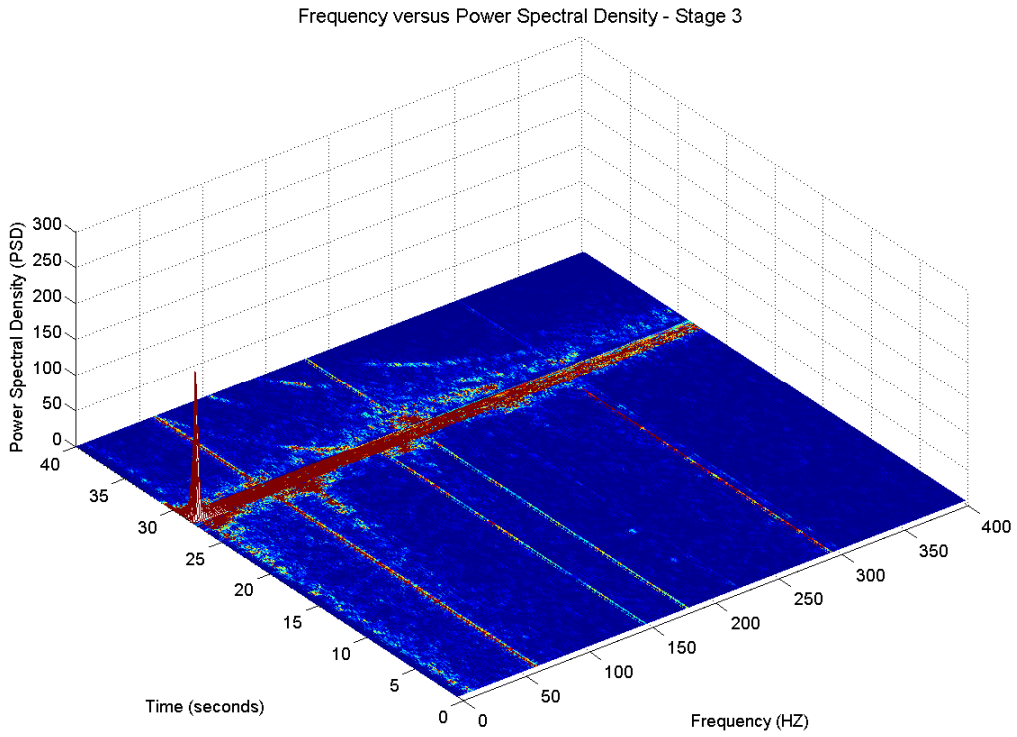

Figure 4. High-Speed Stall Stage 3 Frequency versus Power Spectral Density

The figure takes a sample of 40 seconds of data for a longer time history and thus shows the stall event occurring at approximately 27 seconds. The figure indicated the expected 60 Hz instrument noise, the gas generator rotational frequency of approximately 146 Hz as well as the first harmonic of each of these. By analyzing the expected stall wave at half of rotor speed we can see the stall perturbation occurring before the engine stops. The following figure is a closer view of the stall event highlighting the stall perturbation.

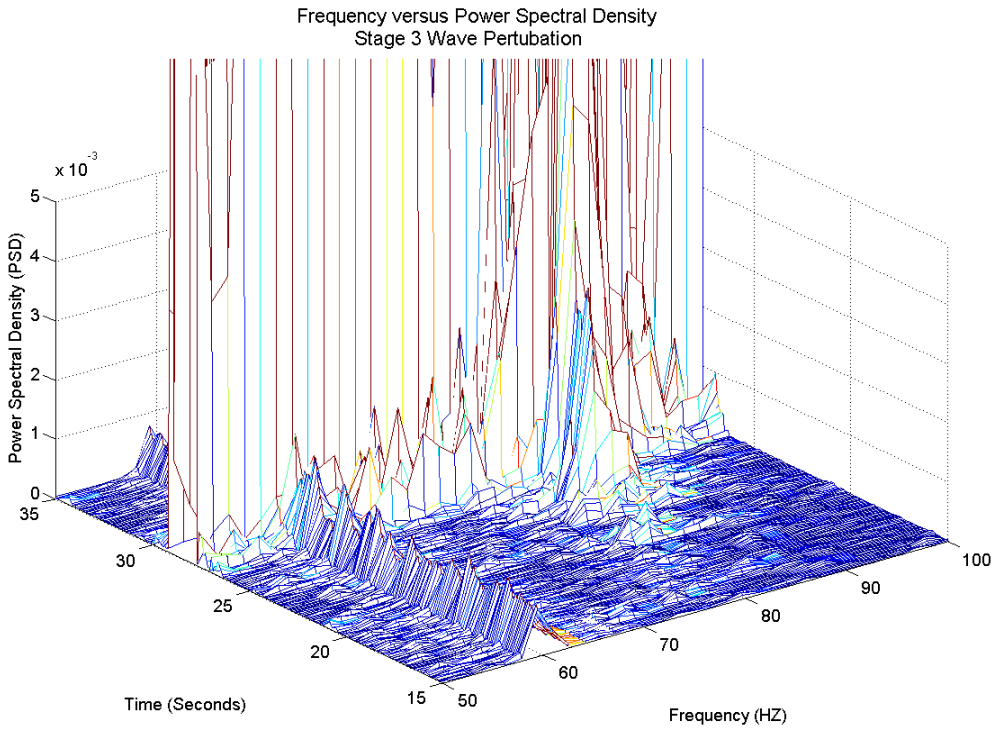

Figure 5. Frequency versus Power Spectral Density Stage 3 Wave Pertubation

The figure shows the perturbation starting at approximately 6 seconds before the stall event occurs at 81.25 Hz or 55.6 percent of rotor speed. The perturbation grows until about 2 seconds before stall when it is at 84.5 Hz or 57.8 percent of rotor speed.

This wave perturbation that occurs is significant because it not only gives advance warning to the stall but it shows this engine running at high speed does indicate the presence of stall precursors. To determine the actual energy growth at these frequencies the Power Spectral Density is plotted versus time.

The following graph is a 100 second interval that averages the PSD values in three different frequency ranges. The ranges chosen were from 80-90 Hz, 75-95 Hz, and 70-100 Hz. The PSD is averaged by taking the sum of the energy at each period of time in the frequency range and dividing it by the number of available points. The purpose of the gradual increase in frequency

range was to determine if a smaller frequency band would have a greater sensitivity to the energy increase. The expected wave perturbation at half rotor frequency should have occurred at approximately 75 Hz, so it would also be beneficial to know if a large enough band would be detrimental to indicating an impending stall.

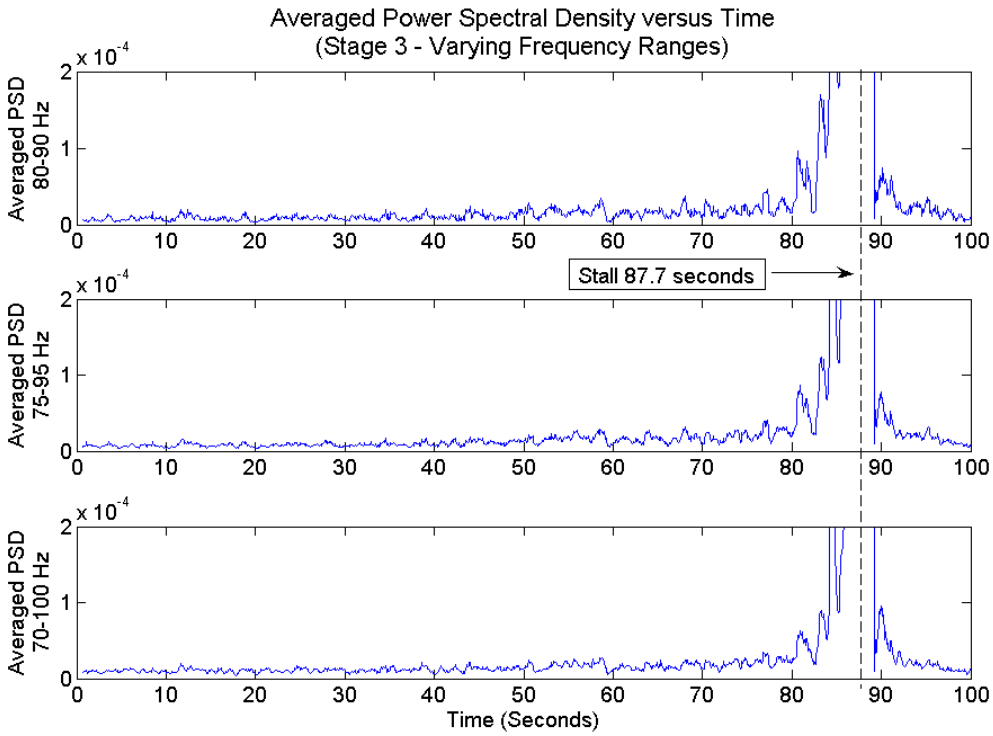

Figure 6. High-Speed Stall Stage 3 Averaged Power Spectral Density versus Time for Varying Frequency Ranges

Figure 6 indicates a gradual increase in the average PSD over the three frequency intervals. The narrower frequency interval centered around the actual wave depicted by the upper graph; however, all three frequency bands do show a significant increase at approximately 81 seconds into this interval. The stall takes place at approximately 87 seconds which would allow for a 6 second notification of the impending stall. This 6 second notification translates into about 880 rotor revolutions. The additional PSD charts for stage 6 and stage 15 can be found in Appendix II.

The above figure indicates for this engine configuration the most sensitive frequency band is the 80-90 Hz band. The three pressure signals are now plotted to determine which pressure signal is better able to see the wave perturbation.

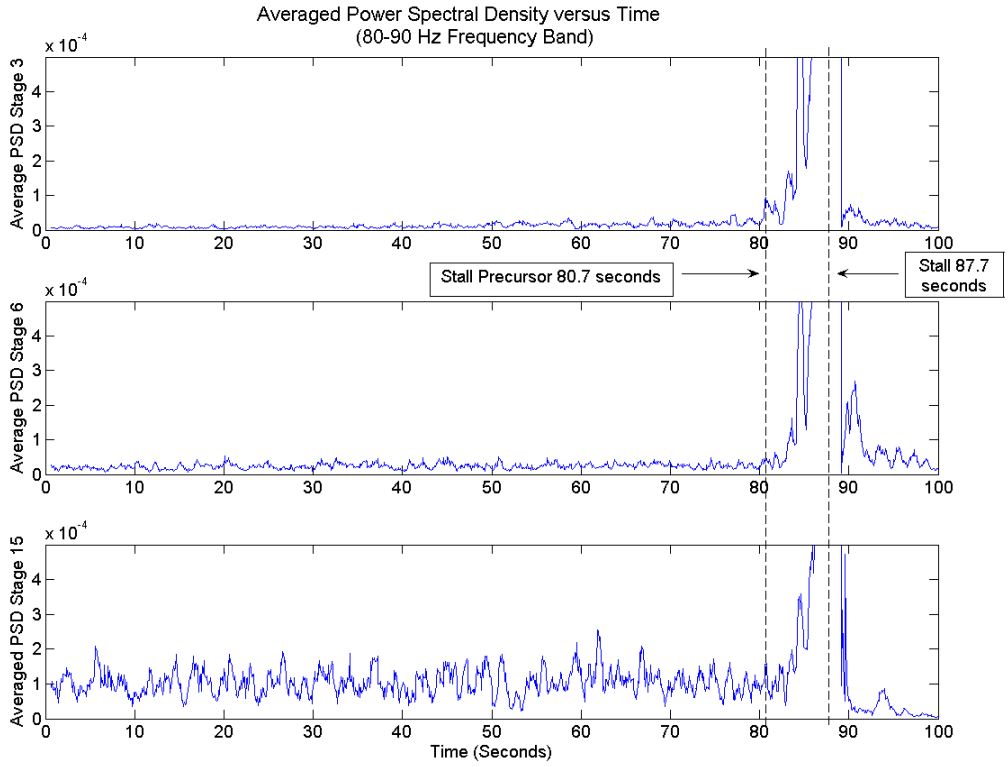

Figure 7. High-Speed Stall Power Spectral Density versus Time for All Stages

Figure 7 above plots the stages from top to bottom with stage 3 on the top and stage 15 on the bottom. The y scales are the same in order of magnitude to adequately compare the three results. The figure shows that the farther the stage is towards the rear of the engine the noisier the signal becomes and the harder it is to distinguish the perturbation as it gradually increases with time. The first pressure signal located at stage 3 has a sharp increase at approximately 81 seconds while Stage 6 and Stage 15 do not show this increase until approximately 84 seconds. This would indicate the pressure sensor located at

stage 3 will be the best available sensor to minimize the noise and increase the likelihood of detecting the wave perturbation.

The analysis up to this point has been done with an FFT size of 32,768 due to the sampling rate of 51.2 kHz. An FFT can distinguish frequencies up to the Nyquist frequency which is one half of the sampling rate. At this sampling rate frequencies up to 25.6 kHz. By utilizing 32,768 points for this frequency range there is enough resolution to accurately see the frequency response in the 80-90 Hz. range. To determine if a smaller sampling rate and smaller FFT size can be used the data was reduced artificially and analyzed. These results are shown in the sensor determination section of this chapter.

3. Correlation Analysis

The final analysis performed on this data was done using an autocorrelation technique. The autocorrelation was performed on every 2000 data points along the time interval evaluated. Every time step analyzed was then summed and averaged over the lag interval of 199 points. This is then plotted versus time to determine the change in the average autocorrelation value.

The figure below illustrates this technique performed on stage 3.

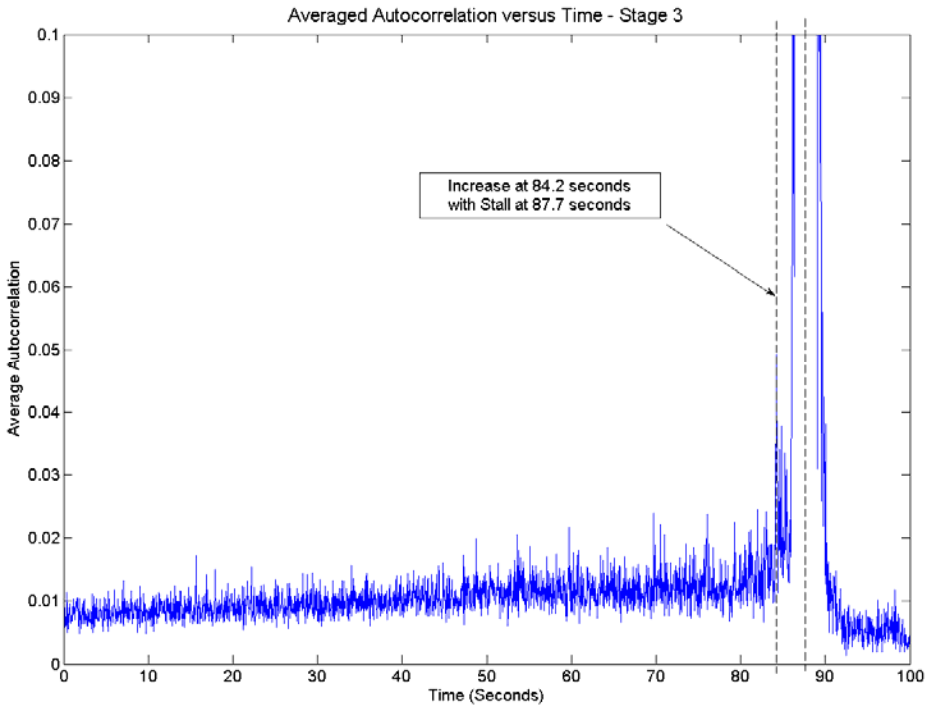

Figure 8. High-Speed Stall Stage 3 Autocorrelation versus Time

The autocorrelation illustrates a rise in values as the engine approaches stall; however, with the autocorrelation the rise does not take place until 24 seconds into the interval. The earlier analysis with PSD showed a gradual increase from 21 seconds onward. The autocorrelation technique, although showing some indications, predicts this three seconds later than the previous PSD analysis.

The autocorrelation figures for stage 6, and stage 15 can be found in Appendix II.

4. Sensor Determination

The previous PSD analysis has shown that at a sampling frequency of 51200 Hz and a large FFT length the pre-stall wave perturbation is detectible up to six seconds before the stall point. The best available sensor due to reduced noise has been shown to be the pressure sensor located at stage 3. This section

will artificially lower the sampling frequency of the sensor and vary the FFT lengths in order to determine the possibility of changing the sampling frequency and FFT lengths.

The sampling frequency was artificially reduced by removing points in the data series to achieve sampling frequencies of 2,048, 6,400, and 12,800 Hz. The lower frequency is large enough to be able to obtain resolutions of frequencies down to the wave perturbation frequency of 80-90 Hz.

The figure below is a plot of all three sampling frequencies with a constant FFT length of 1,024.

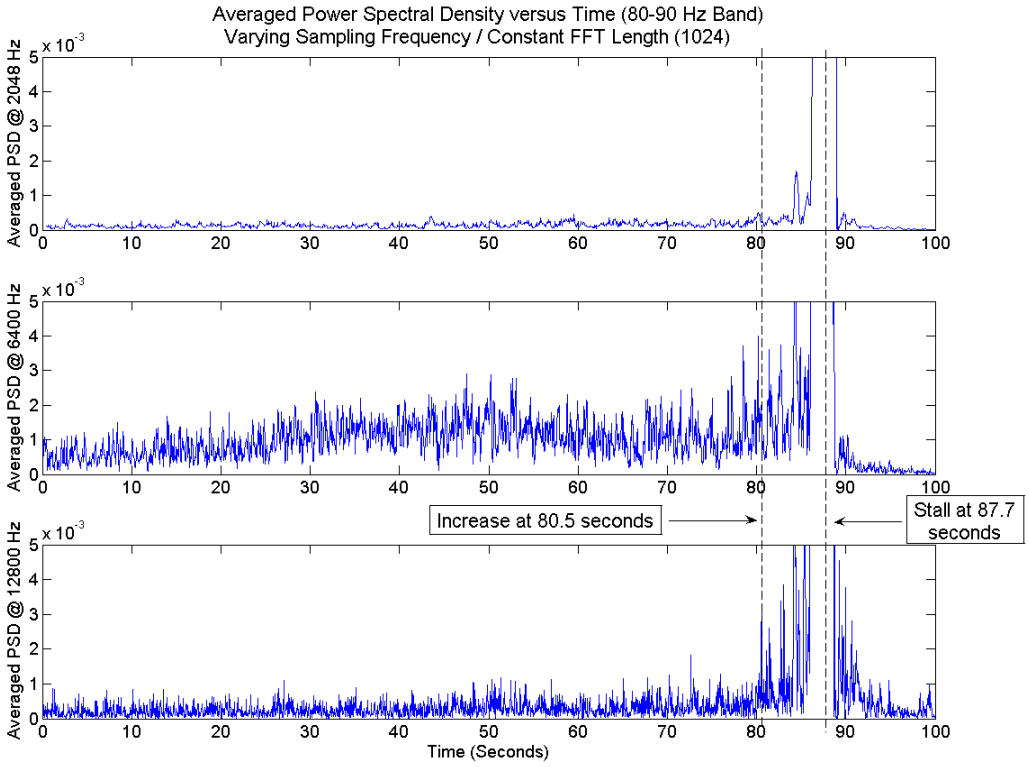

Figure 9. Average Power Spectral Density versus Time Varying Sampling Frequency / Constant FFT Length of 1024

The figure illustrates that at the lower sampling frequencies of 2,048 and 6,400 the rise in power spectral density can not be determined; however, at the sampling frequency 12,800 the increase in power spectral density can be determined at approximately 81 seconds or 6 seconds before the stall event.

The following figure is based on a constant sampling frequency of 12,800 Hz while varying the FFT length.

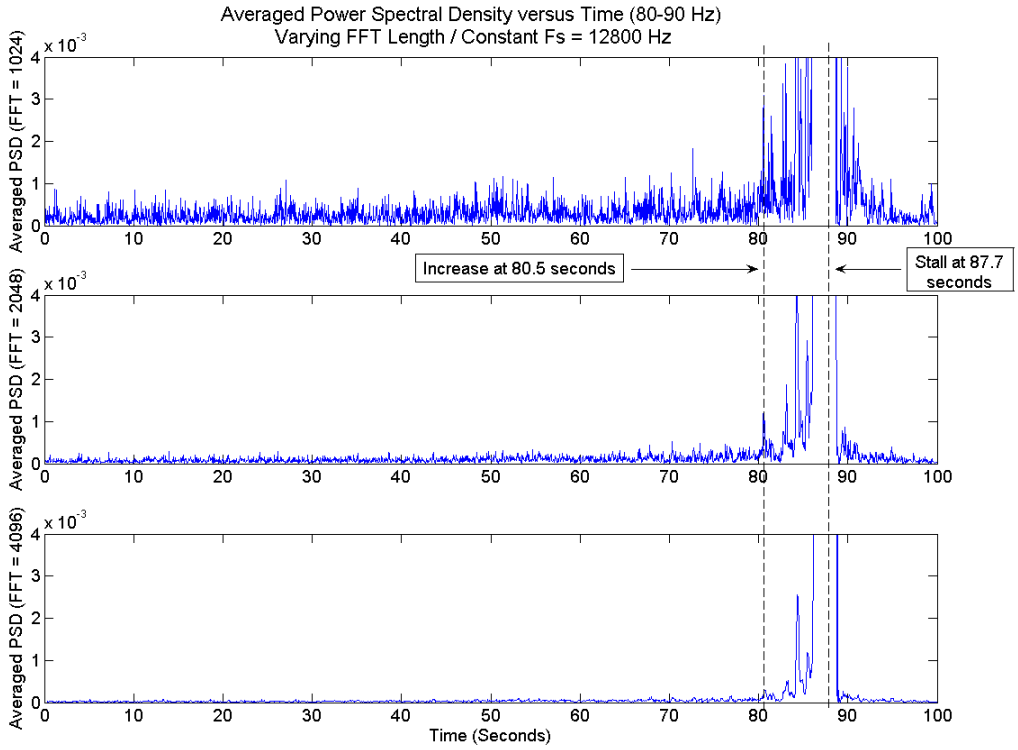

Figure 10. Average Power Spectral Density versus Time for a Constant Sampling Frequency of 12,800 Hz

This figure illustrates that the rise in power spectral density at 12,800 Hz can be determined by utilizing any FFT length from 1,024 to 4,096. Each FFT shows a sharp increase at approximately 81 seconds into this interval.

The additional plots for varying FFT length versus varying sampling frequency can be found in Appendix II.

C. FLAMEOUT TRIP

The analysis of the high speed data run showed that there was a pre-stall wave perturbation at approximately half of rotor speed. The results of the flameout trip were done utilizing the same techniques to determine if a wave perturbation developed during this engine run.

The flameout trip data run was performed at a gas generator speed of 7000 RPM or 116.6 Hz. There were no audible indications of a stall in the control room when the engine tripped.

1. Analysis

The following figure illustrates the Power Spectral Density versus Frequency for this engine run.

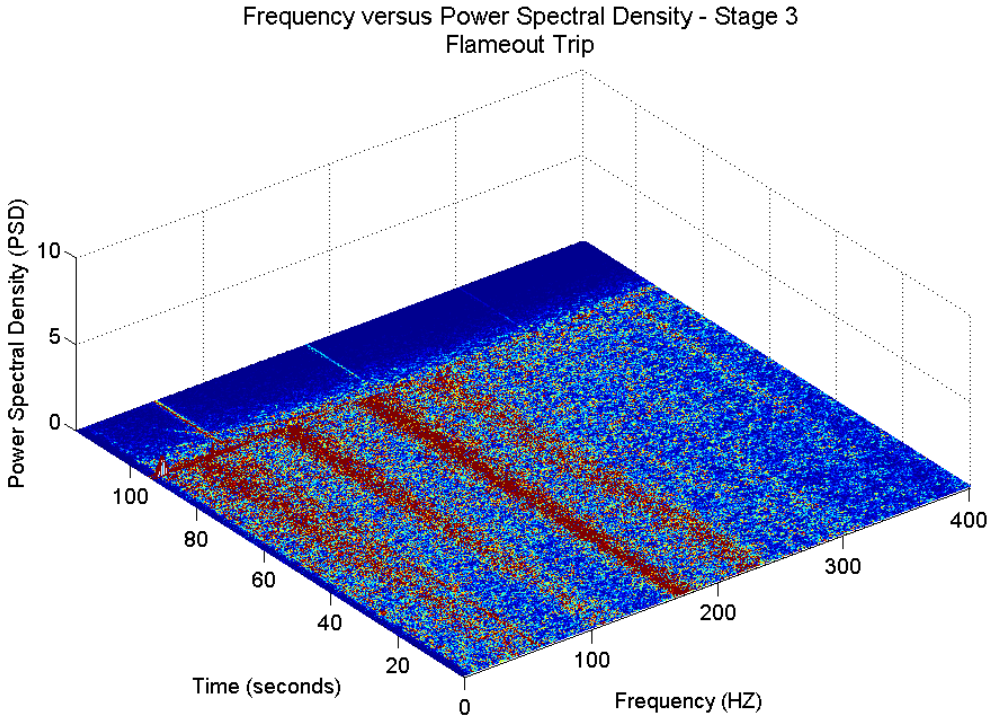

Figure 11. Flame Out Trip Stage 3 Frequency versus Power Spectral Density

The figure shows a gradual increase in the Power Spectral Density from 90-120 Hz. The pre-stall wave perturbation given that the rotor speed is 116.6 Hz should be located at approximately 60 Hz. The following figure shows an enhanced view of the low frequencies before the engine trips.

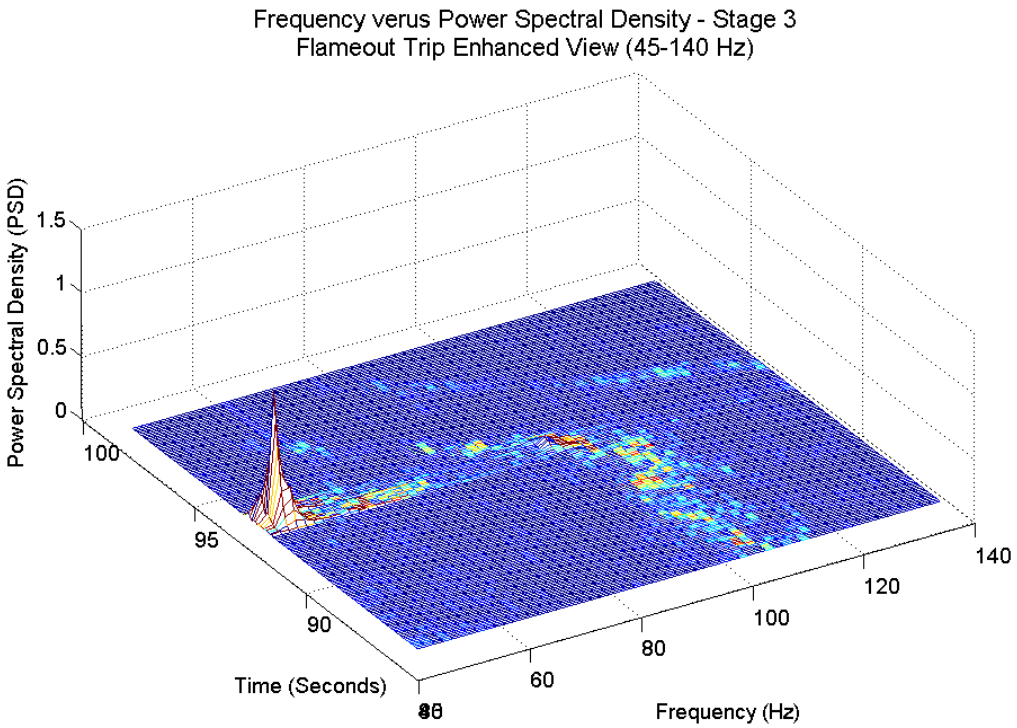

Figure 12. Flame Out Trip Stage 3 Enhanced view around 60 Hz

Utilizing the 60 Hz frequency line as a guide and just prior to the engine tripping we can not ascertain a pre-stall wave forming. The frequency range from 90-120 Hz, around rotor frequency; however, does show a gradual rise in energy prior to the trip.

The following figure looks at the Power Spectral Density from 90-120 Hz and is plotted this versus time.

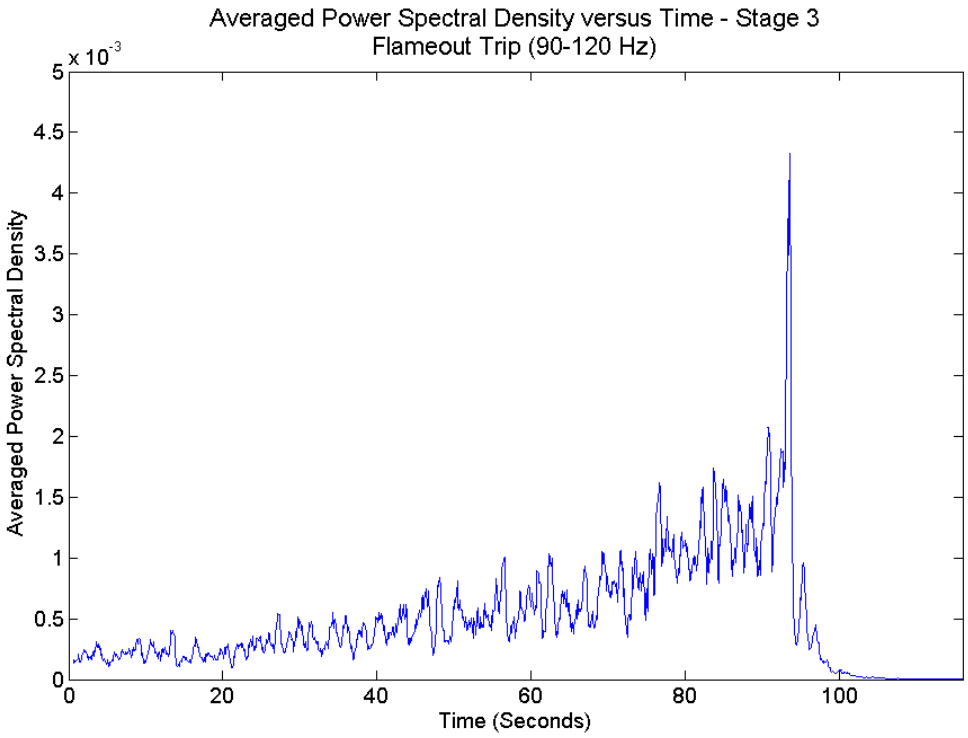

Figure 13. Flameout Trip Stage 3 Power Spectral Density from 90-120 Hz

The figure illustrates that at the beginning of the interval for the available data the energy was relatively flat, but at approximately 20 seconds the energy started to increase to the engine trip point.

The following figure is the autocorrelation plot versus time for this engine run.

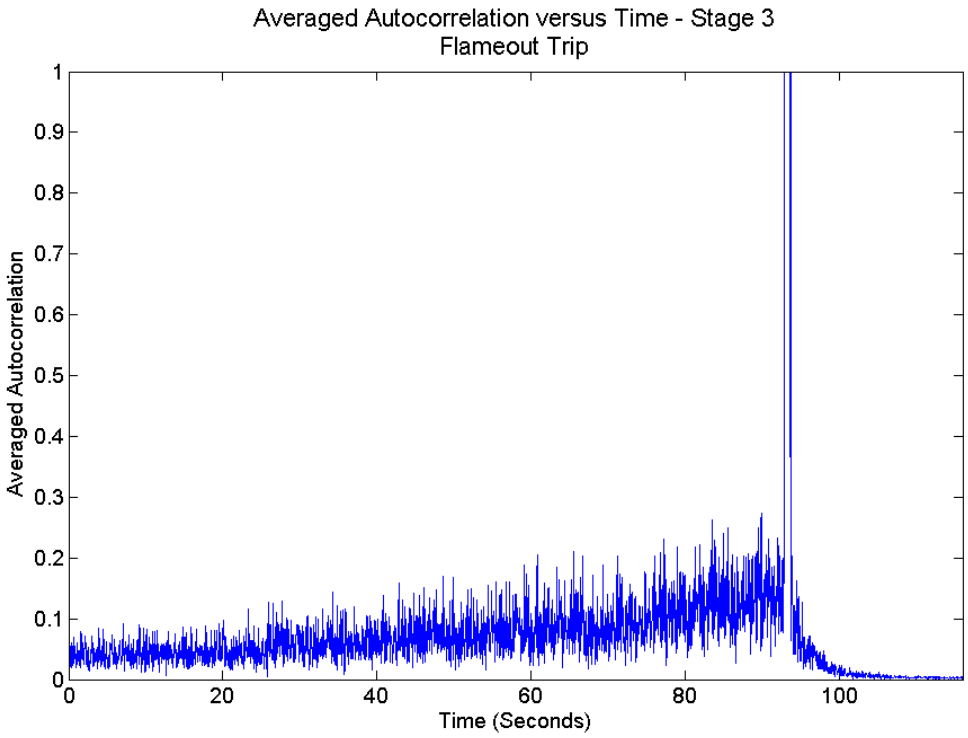

Figure 14. Flameout Trip Stage 3 Autocorrelation versus Time

The autocorrelation for this data also illustrates the gradual rise to the engine trip point as the power spectral density plot has shown.

2. Data Run Conclusion

The Flameout Trip engine run did not show an indication of a stall wave perturbation; however, there is indication of a gradual rise in spectral energy that could be used to give advance warning of an engine trip.

D. HIGH VIBRATION TRIP

The high vibration trip engine run was performed at a gas generator speed of 7500 RPM or 125 Hz. There were no audible indications of a stall in the control room when the engine tripped.

1. Analysis

The following figure is the PSD versus Frequency plot of this engine run.

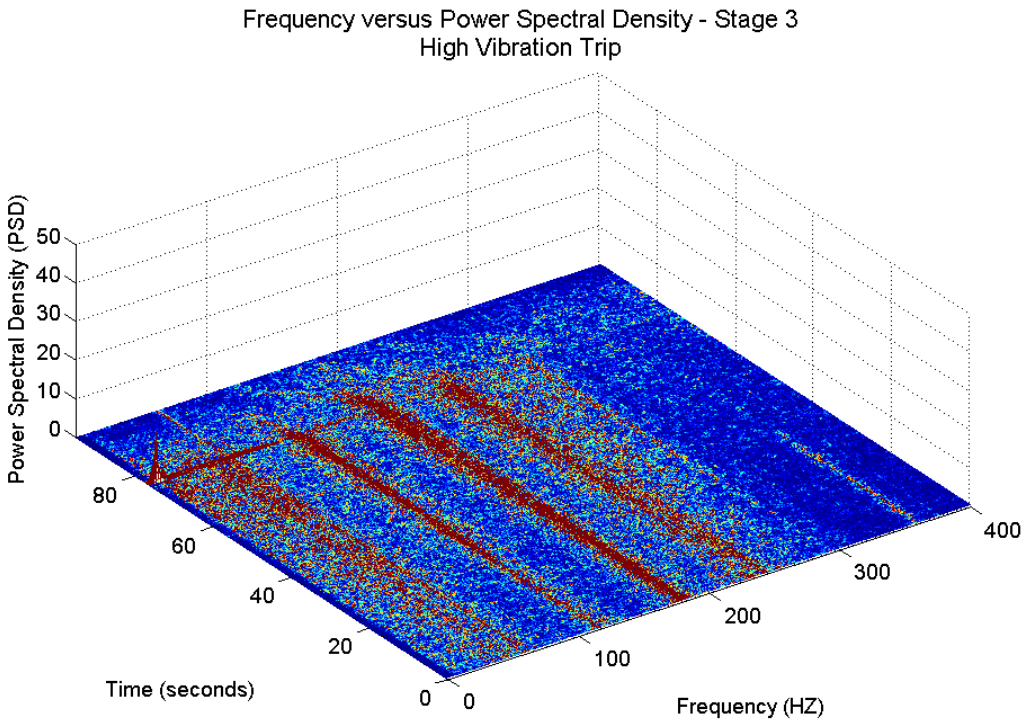

Figure 15. High Vibration Trip Stage 3 Frequency versus PSD

The overview of this frequency spectrum shows a gradual increase in energy around the gas generator rotor speed similar to the flameout trip engine run.

The following figure is a closer view of the lower frequencies.

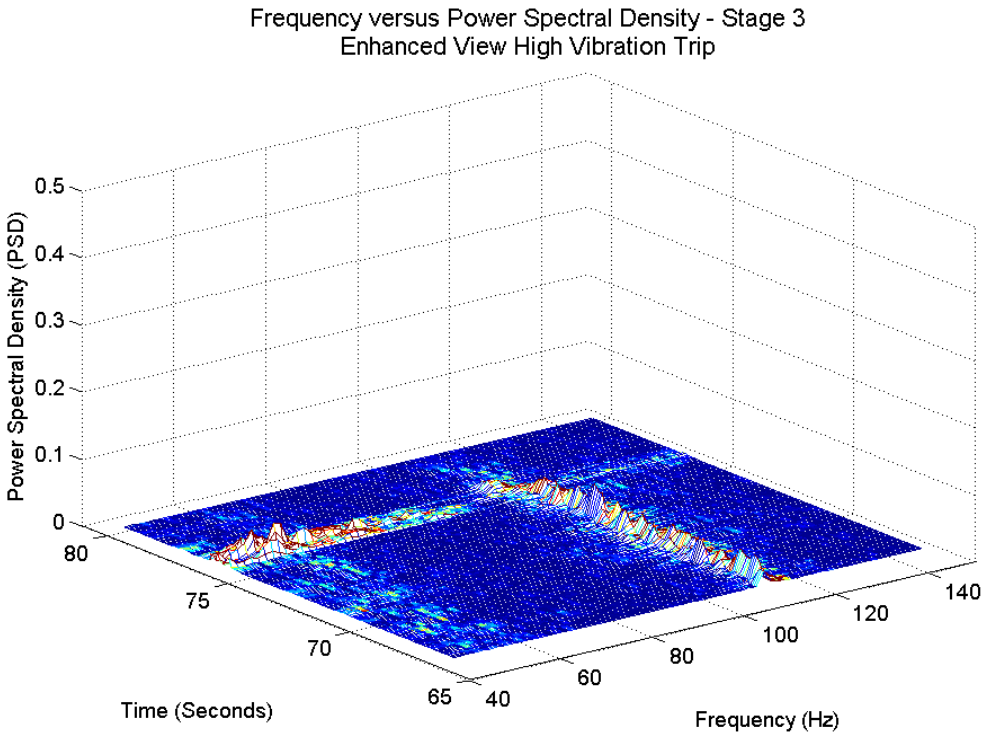

Figure 16. High Vibration Trip Stage 3 Frequency versus PSD Close View

The expected wave at approximately half rotor speed is not here for this data run although as mentioned just below rotor speed there is a gradual increase in energy up until the point of engine trip.

The following is an average PSD versus time for a frequency range of 90-120 Hz.

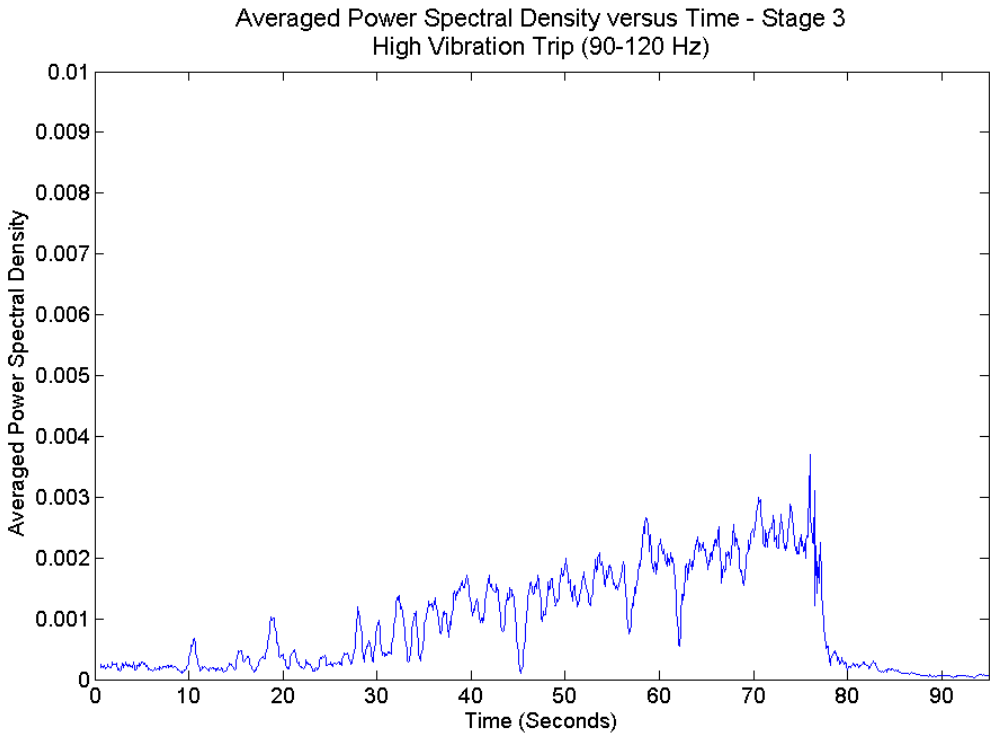

Figure 17. High Vibration Trip Stage 3 Average Power Spectral Density versus Time

Prior to the ten second mark on this graph the PSD is rather flat. At approximately the twenty second mark onward you see a gradual increase in energy until the engine trips.

The autocorrelation graph is shown below.

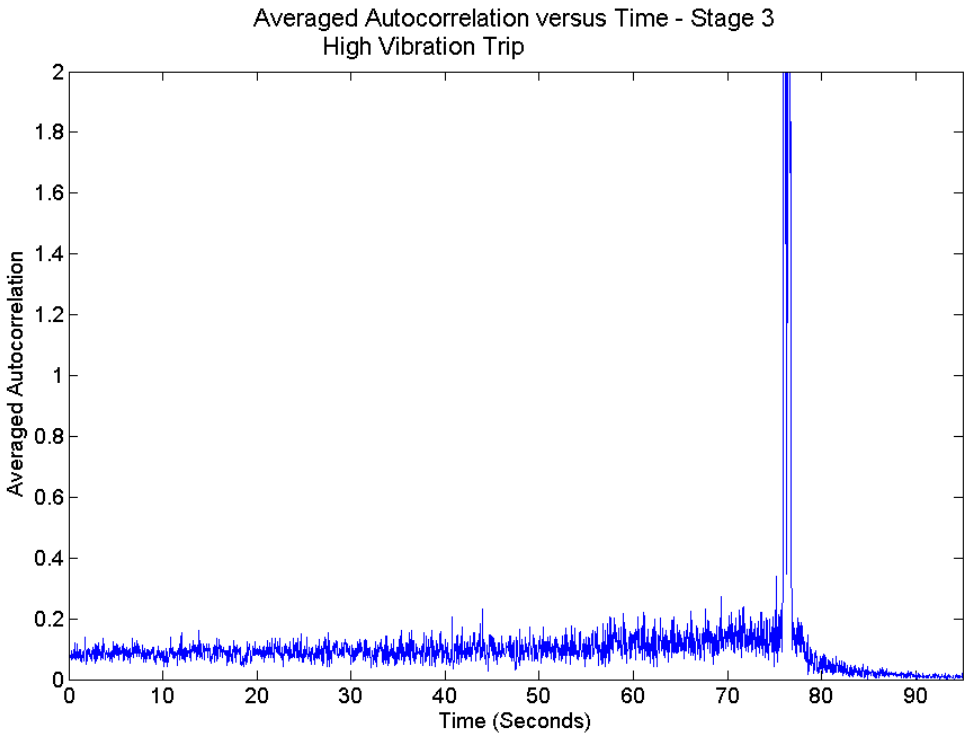

Figure 18. High Vibration Trip Stage 3 Averaged Autocorrelation versus Time

The autocorrelation plot also shows a slight increase until the engine stops.

2. Engine Run Results

This engine run produced no indication of pre-stall wave perturbations as would be expected around half rotor speed; however, there is an indication of increased spectral energy that could be used for engine trip notification.

E. ENGINE TRIP

The engine trip data engine run was performed at an unknown gas generator speed. There were no audible indications of a stall in the control room when the engine tripped.

1. Analysis

The first figure is the frequency versus PSD for this data run.

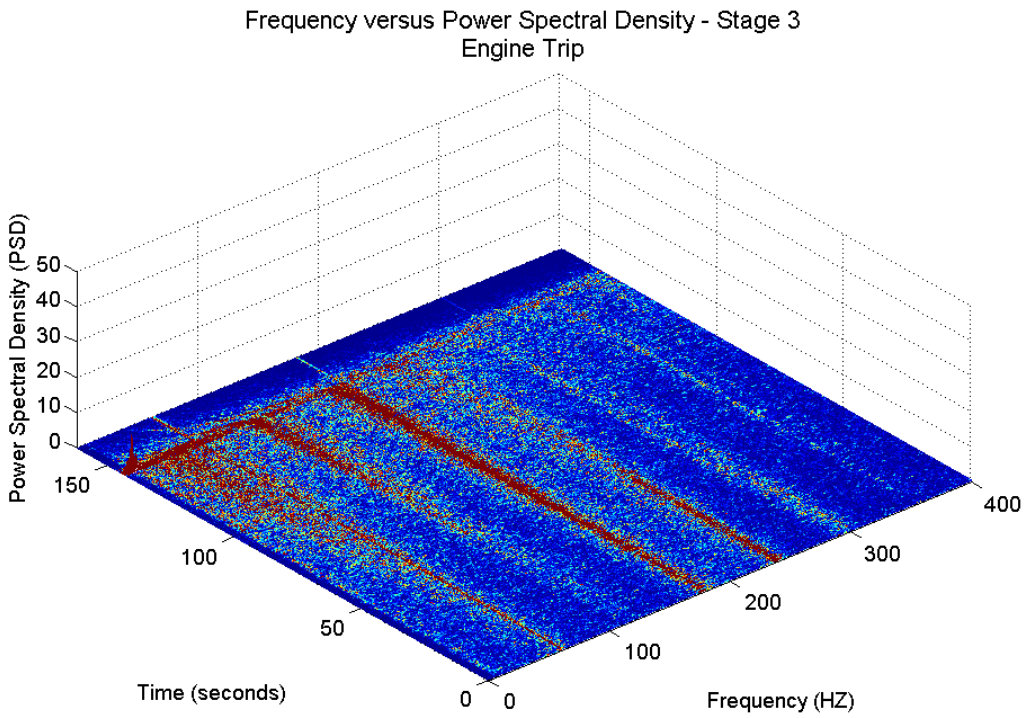

Figure 19. Engine Trip Stage 3 Frequency versus Power Spectral Density

The figure illustrates a similar increase in energy at slightly below the gas generator speed. The following figure will show a closer view of the lower frequencies just prior to the engine tripping.

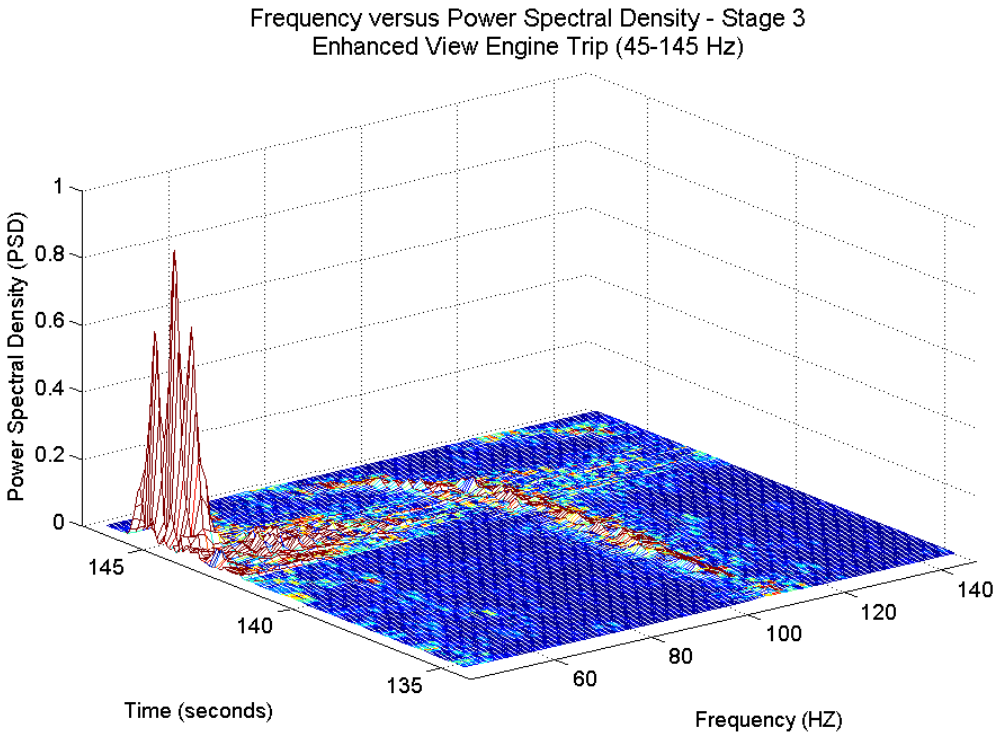

Figure 20. Engine Trip Stage 3 Frequency versus Power Spectral Density Closer View

The figure does not show a wave perturbation at half or rotor speed; however, there is an increase in energy similar to the previous two engine runs. The following figure will plot the PSD for a frequency range of 90-120 Hz.

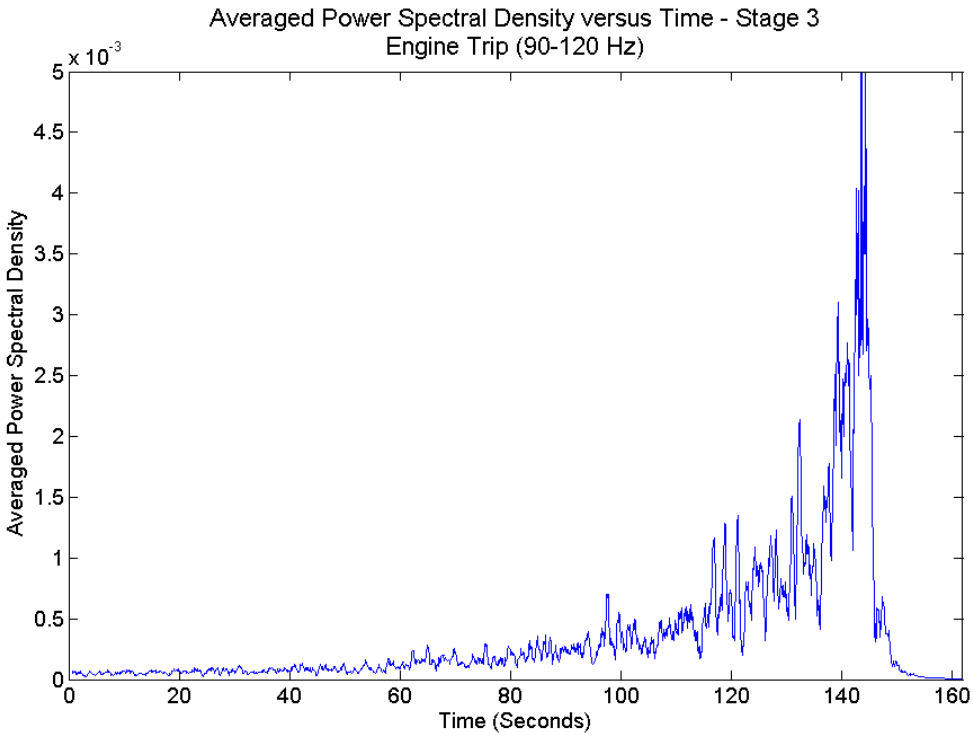

Figure 21. Engine Trip Stage 3 Averaged Power Spectral Density versus Time

The averaged power spectral density shows a gradual increase up until the engine tripping. The following figure is the autocorrelation plot versus time for this same time interval.

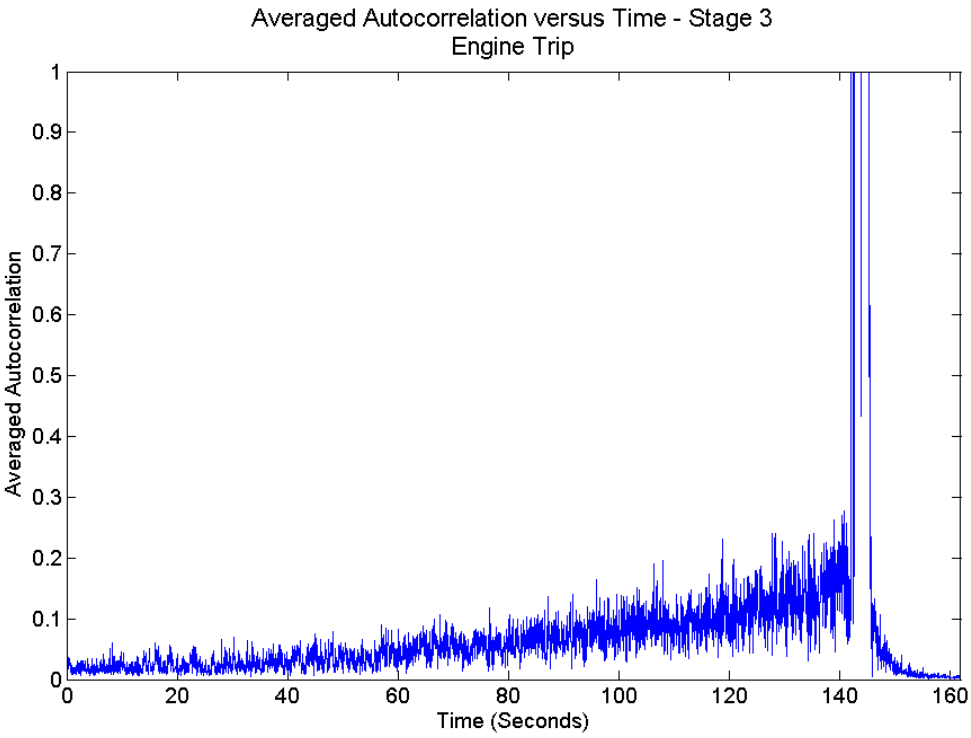

Figure 22. Engine Trip Stage 3 Autocorrelation versus Time

The autocorrelation plot also reveals the same gradual increase until the engine trips.

The additional plots for stage 6 and stage 15 can be found in Appendix II.

2. Engine Run Conclusion

This engine run produced similar results as the previous two flameout trip, and high vibration trip runs. The gradual increase can give an indication of the engine tripping; however, there is no indication of pre-stall wave perturbations.

V. CONCLUSIONS

Signal processing was performed on all four data runs that were provided for the LM-2500 gas turbine. Based on the results of processing the following conclusions can be drawn that address the initial objectives that were set:

- The fast Fourier transform analysis was performed on the data from the LM-2500 gas turbine and stall wave perturbations were detected.
- The Power Spectral Density was on the resulting fast Fourier Transform and a pre-stall modal oscillation can be seen at approximately one half of rotor speed before the engine stalls.
- A correlation analysis was performed that does show that effects of this modal oscillation.
- Stall precursor were found at 81.25 Hz in the high-speed data run. The stall precursor started at 55.6 percent of rotor speed. The best available sensor for this modal detection is the pressure sensor located at stage 3. This sensor should sample at a rate of at least 12.8 kHz and be analyzed through a fast Fourier transform with at least 1,204 points.

THIS PAGE INTENTIONALLY LEFT BLANK

APPENDIX I. MATLAB CODE

A. TIME SERIES CODE

The following code was used to generate the time series plots of pressure versus time.

```
% Gustave C. Dahl - Thesis Work
% Real Time Plot of Pressure
%
%  Track1 - VM Stage 4
%  Track2 - VM Stage 7
%  Track3 - WM Stage 15

clear tlength datal s t x2 j Track1Short Track2Short Track3Short
Track4Short xshort;

% Set initial known values or inputed values
    % Length Of Track in Seconds
        tlength = 20;
    % Data Point Iteration (Used to reduce plot clutter)
        datal = 40;
    % Define Start/Stop Plot Interval (Used to focus on specific time)
        plotstart = 0;
        plotstop = 20;

% Create Our Time Vector

s = length(Track1);
t = linspace(0,20,s);

% Initiate Values

x2(1) = 0;
j=1;

% Loop through to reduce vectors

for i=2:1:s/datal
    x2(i)=x2(i-1)+datal;
end

for i=0:1:s;
    if i == x2(j)
        Track1Short(j)=Track1(i+1);
        Track2Short(j)=Track2(i+1);
        Track3Short(j)=Track3(i+1);
        Track4Short(j)=Track4(i+1);
        xshort(j)=t(i+1);
        j = j+1;
    end
    %Quit looping to avoid calling undefinded object
```

```
    if j>length(x2)
       break
    end
end

% Added to plot interval of time
    % Points Per Second
    points = length(xshort)/tlength;
    % Define start and stop data points
    pointstart = round(plotstart * points);
    pointstop = round(plotstop * points);


% Plot Pressure Plots For All Tracks
subplot(3,1,1)
plot(xshort(pointstart:pointstop),Track1Short(pointstart:pointstop))
title(RecordDate)
ylabel(Track1_Name)
xlim([plotstart plotstop])
hold on;
subplot(3,1,2)
plot(xshort(pointstart:pointstop),Track2Short(pointstart:pointstop))
ylabel(Track2_Name)
xlim([plotstart plotstop])
subplot(3,1,3)
plot(xshort(pointstart:pointstop),Track3Short(pointstart:pointstop))
ylabel(Track3_Name)
xlim([plotstart plotstop])
xlabel('Time (Seconds)')
```

B. FFT / PSD CODE

This code was used to calculate the FFT versus PSD plots generated for this analysis.

```
%  Gustave C. Dahl - Thesis Work
%  FFT and Power Spectral Analysis
%
%  Start Clock / Clear Values
tic
clc
clear Fs Fn t1 t2 y2 t NFFT NFFT_int iter NumUniquePts x i FFTX1 FFTX
MX f f2 z MXmax1 MXmax2 MXmax3 MXmax1n MXmax2n MXmax3n int1l int1h
ACdata1 ACdata2 ACdata3 ACs1 ACs2 ACs3
%------------------------------
%Set Initial Values
%------------------------------
ovl = 8;             % Overlap Desires (Fraction of 1)
tl = 40;            % Input Track Length (Seconds)
NFFT = 2^15          % FFT Length
track = Track140;    % Called Track Data
Fs=51200;            % Sampling Freqency
Fn=Fs/2;             % Nyquist Frequency
maxf = 400;          % Max Required Frequency
```

```
    % The following values are used to plot the average PSD over a
Specifc
    % Frequency Range
        fint1lw = 70;
        fint1ln = 75;
        fint1l = 80;
        fint2h = 90;
        fint2hn = 95;
        fint2hw = 100;

%-------------------------------
% Calculate Initial Values
%-------------------------------
NFFT_int = fix(NFFT/ovl);
tl_int = ((NFFT/(length(track)/tl))/ovl);
tl_start = tl/(length(track)/NFFT);
loop_int = floor(tl/tl_int);
NumUniquePts = ceil((NFFT+1)/2);
%-------------------------------
% Loop Through to obtain FFT and PSD Values
%-------------------------------
for i=1:1:(loop_int-ovl)

    if i == 1
        x = track(1:NFFT);
        % Freq Max and Mins
            f1=(0:NumUniquePts-1)*2*Fn/NFFT;
            f2(1,:) = f1;
            freq = fix(f2(1,:));
            max = find(freq > maxf);
            intlw = find(freq > fint1lw);
            intln = find(freq > fint1ln);
            intl = find(freq > fint1l);
            inth = find(freq > fint2h);
            inthn = find(freq > fint2hn);
            inthw = find(freq > fint2hw);
            maxfreq = max(1);
            int1lw = intlw(1);
            int1ln = intln(1);
            int1l = intl(1);
            int1h = inth(1);
            int1hn = inthn(1);
            int1hw = inthw(1);
        % Calculate Time
        t(i) = tl_start;
    else
        x = track((NFFT_int*(i-1)):((NFFT_int*(i-1))+NFFT-1));
        t(i) = tl_start+(tl_int * (i-1));
    end

    % Calculate FFT
    FFT1=fft(x,NFFT);
    % Symmetry (Reduce by Half)
    FFT=FFT1(1:NumUniquePts);
    % Magnitude (PSD)
    PSD1=FFT.*conj(FFT)/NFFT;
```

```
    % Multiply by two because we reduced by half
    PSD1=PSD1*2;
    % Normalize to Length of Sample
    PSD1=PSD1/length(x);
    PSD(i,1:maxfreq) = PSD1(1:maxfreq);

    % Frequency
    f1=(0:NumUniquePts-1)*2*Fn/NFFT;
        % Only keep the required frequencies
        f(i,1:maxfreq) = f1(1:maxfreq);

    % Sum PSD Over Frequency Bands and Divide by Points
        PSDA1(i) = (sum(PSD(i,int1l:int1h)))/(int1h-int1l);
        PSDA2(i) = (sum(PSD(i,int1ln:int1hn)))/(int1hn-int1ln);
        PSDA3(i) = (sum(PSD(i,int1lw:int1hw)))/(int1hw-int1lw);

end
toc

figure
mesh(f,t,PSD)
caxis([0 .015])
axis([0 maxf 0 tl 0 3])
xlabel('Frequency (HZ)')
ylabel('Time (seconds)')
zlabel('Power Spectral Density (PSD)')
title('Frequency vs. PSD')
figure
plot(t,PSDA1,'r')
hold
plot(t,PSDA2,'b')
plot(t,PSDA3,'g')
axis([0 tl 0 .2])
xlabel('Time (seconds)')
ylabel('Power Spectral Density')
title('Average Power Spectral Density')
```

C. AUTOCORRELATION CODE

```
%  Gustave C. Dahl - Thesis Work
%  Cross-Correlation Analysis
%
%  Start Clock / Clear Values
tic
clc
clear ACS t NFFT NFFT_int x i AC1
%------------------------------
%Set Initial Values
%------------------------------
ovl = 1;            % Overlap Desires (Fraction of 1)
tl = 40;            % Input Track Length (Seconds)
NFFT = 2000         % Length of Sample
track = Track340;   % Called Track Data
%------------------------------
```

```
% Calculate Initial Values
%-------------------------------
NFFT_int = fix(NFFT/ovl);
tl_int = ((NFFT/(length(track)/tl))/ovl)
tl_start = tl/(length(track)/NFFT)
loop_int = floor(tl/tl_int);
maxlags = 99;
y = linspace(-maxlags,maxlags,199);
%-------------------------------
% Loop Through to obtain FFT and PSD Values
%-------------------------------
for i=1:1:(loop_int-ovl)

    if i == 1
        x = track(1:NFFT);
        t(i) = tl_start;
    else
        x = track((NFFT_int*(i-1)):((NFFT_int*(i-1))+NFFT-1));
        t(i) = tl_start+(tl_int * (i-1));
    end

    AC1 = xcorr(x,maxlags,'unbiased');
    ACS(i) = sum(AC1)/maxlags;


end
toc

plot(t,ACS)
axis([0 tl 0 .1])
xlabel('Time (seconds)')
ylabel('Average Corss-Correlation')
title('Averaged Cross-Correlation')
```

THIS PAGE INTENTIONALLY LEFT BLANK

APPENDIX II. ADDITIONAL FIGURES

A. FFT VERSUS PSD FIGURES

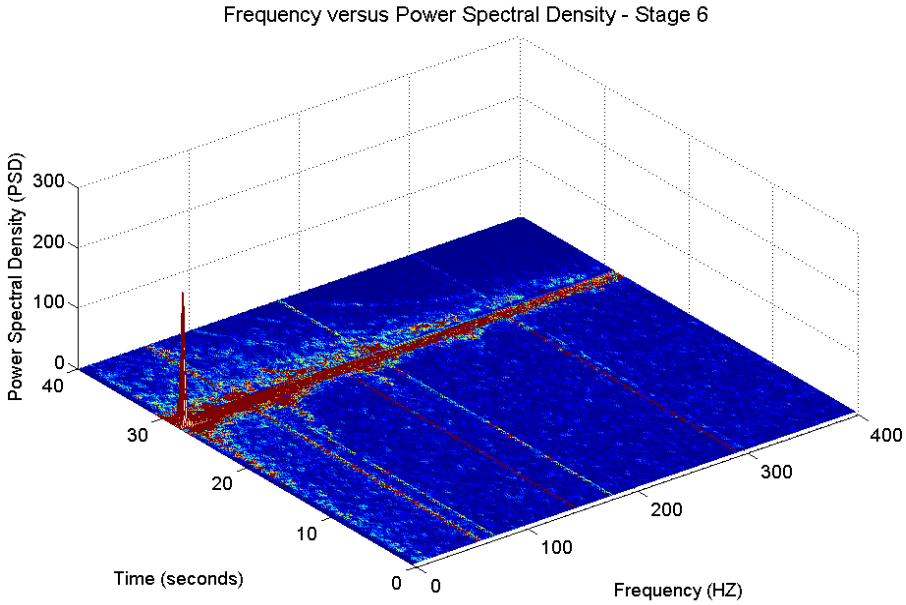

Figure 23. High-Speed Stall Stage 6 Frequency versus Power Spectral Density

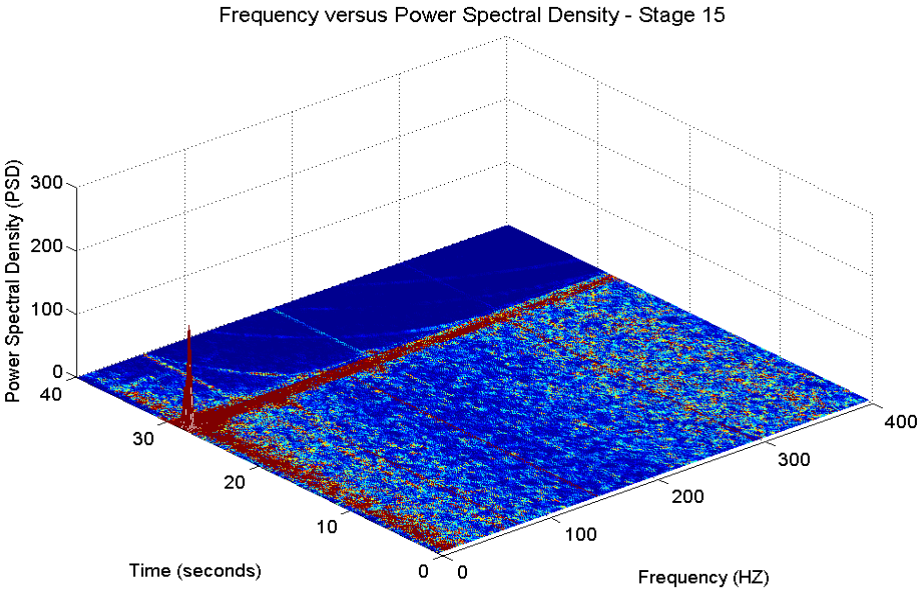

Figure 24. High-Speed Stall Stage 15 Frequency versus Power Spectral Density

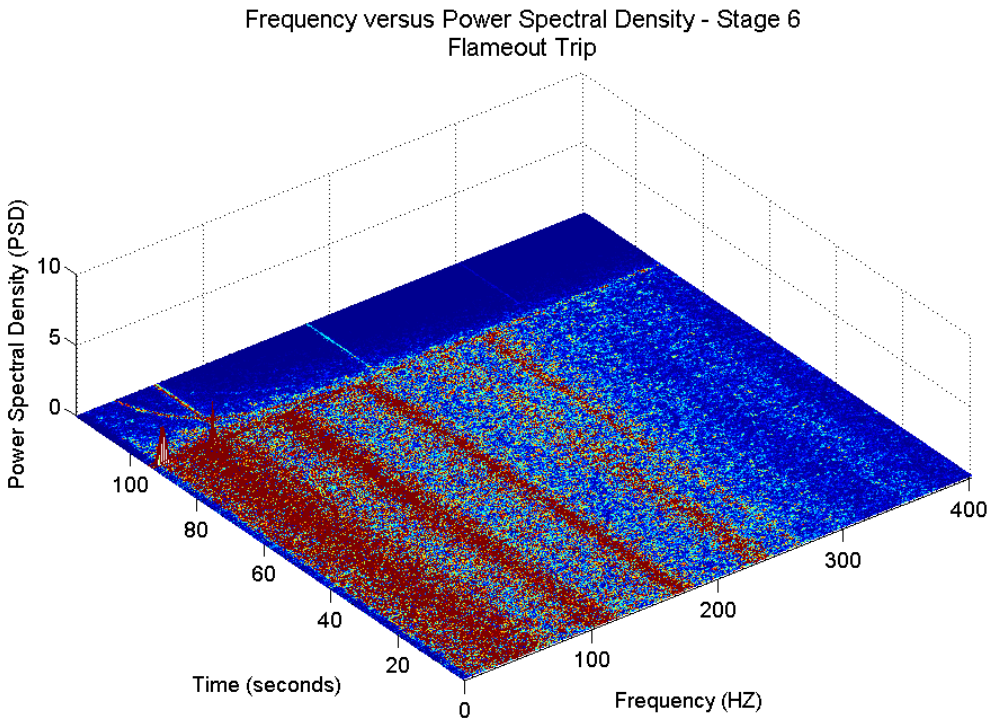

Figure 25. Flameout Trip Stage 6 Frequency versus Power Spectral Density

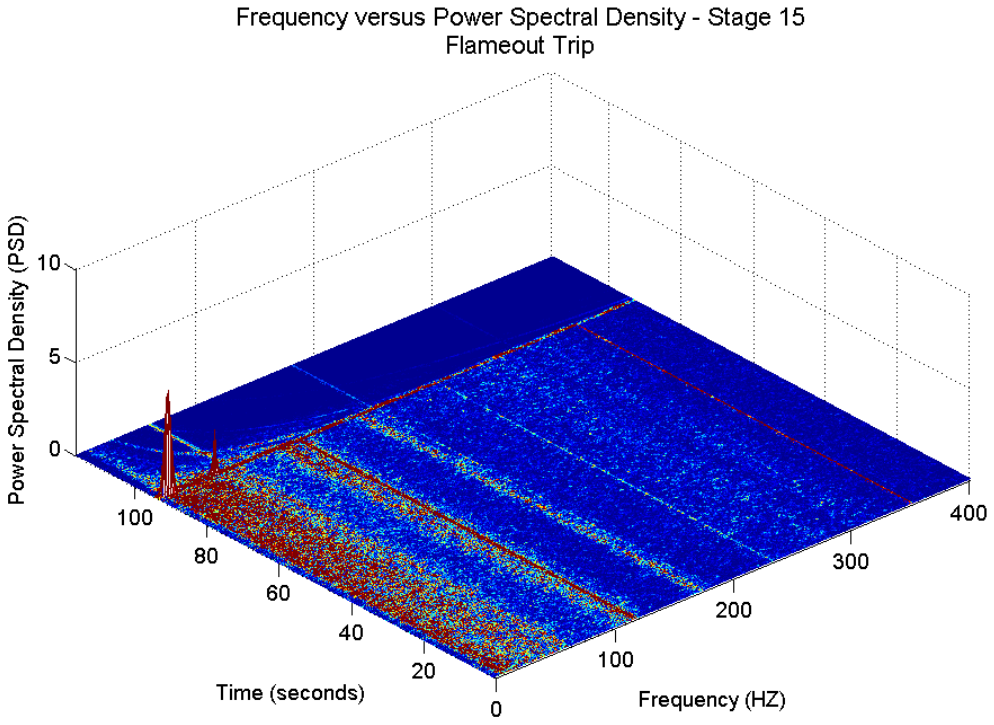

Figure 26. Flameout Trip Stage 15 Frequency versus Power Spectral Density

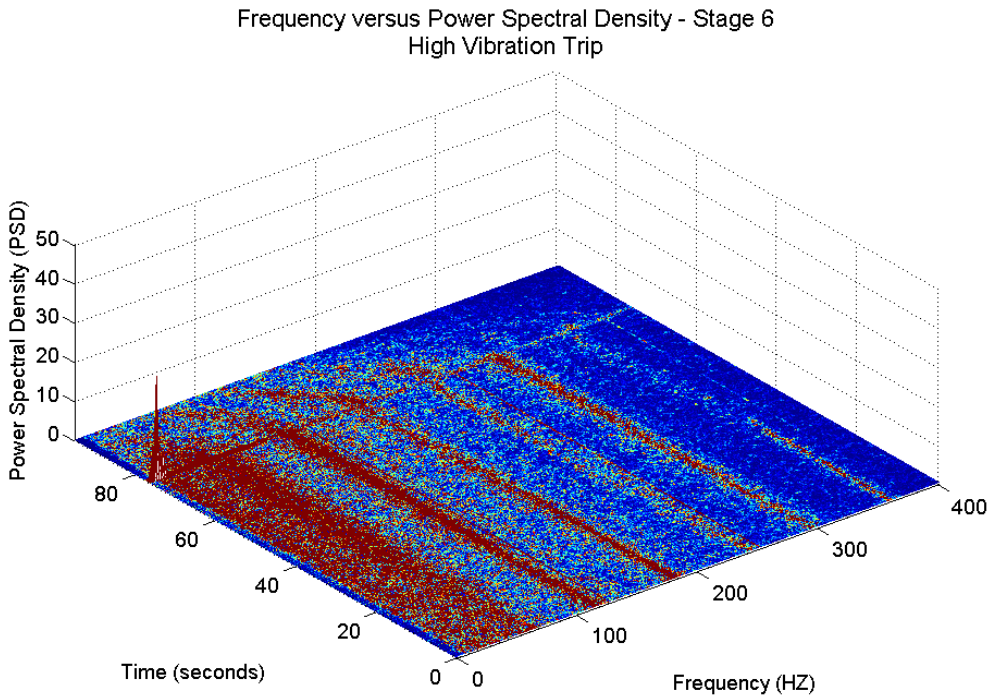

Figure 27. High Vibration Trip Stage 6 Frequency versus Power Spectral Density

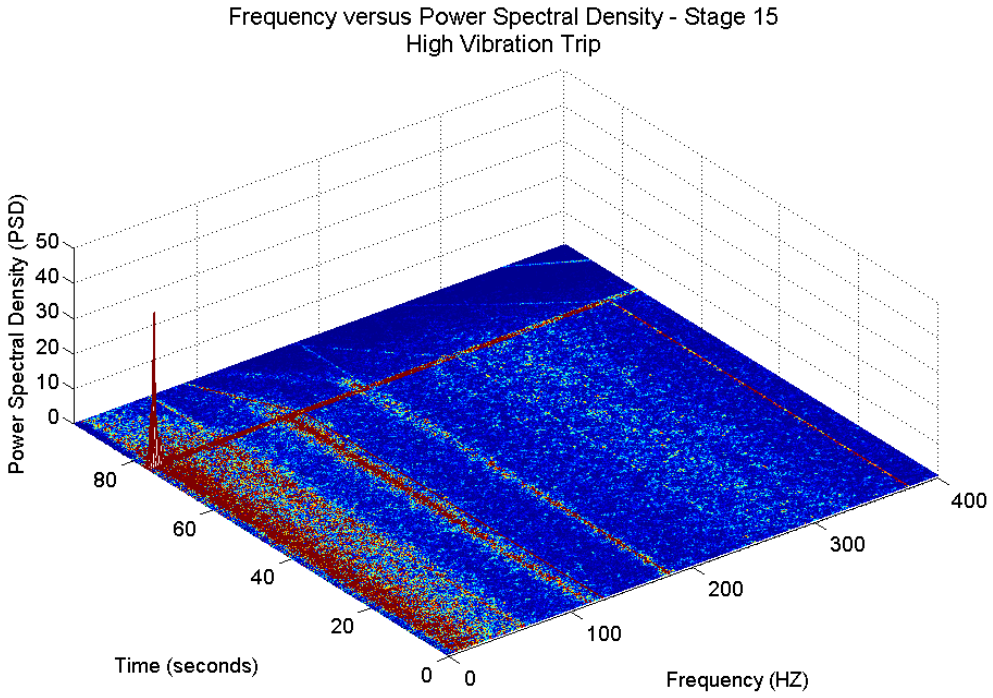

Figure 28. High Vibration Trip Stage 15 Frequency versus Power Spectral Density

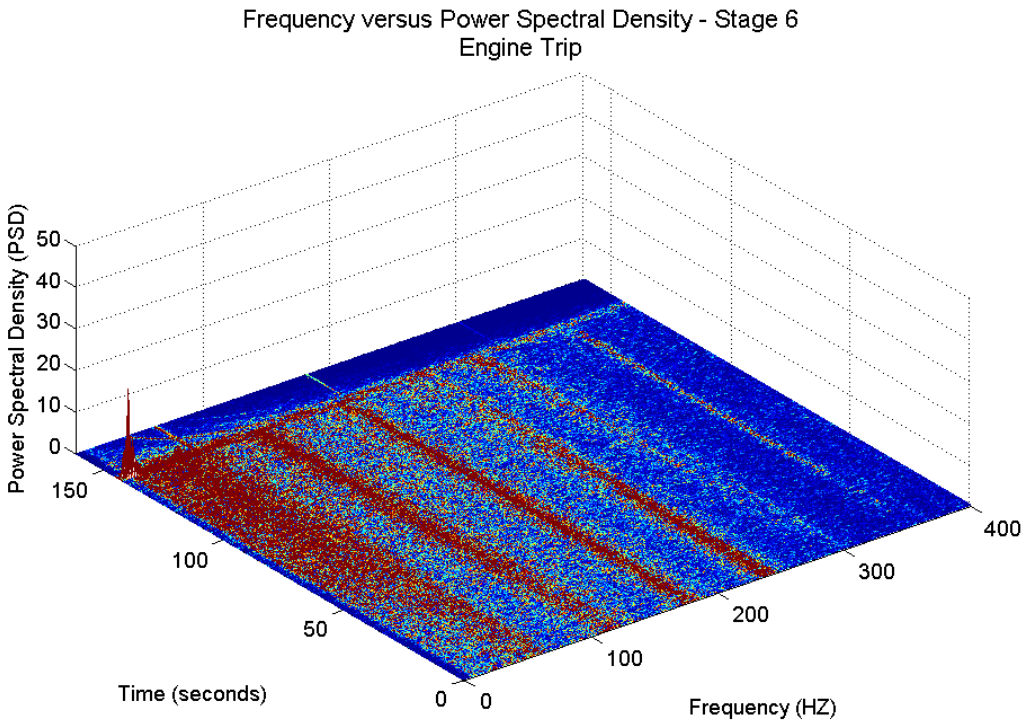

Figure 29. Engine Trip Stage 6 Frequency versus Power Spectral Density

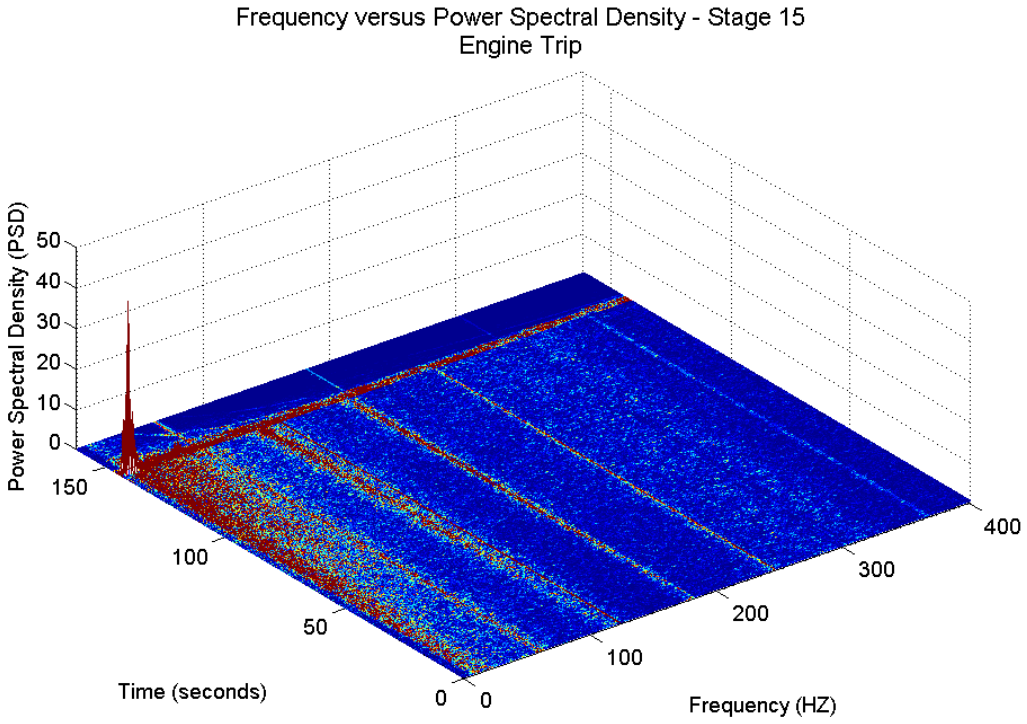

Figure 30. Engine Trip Stage 15 Frequency versus Power Spectral Density

B. PSD FIGURES

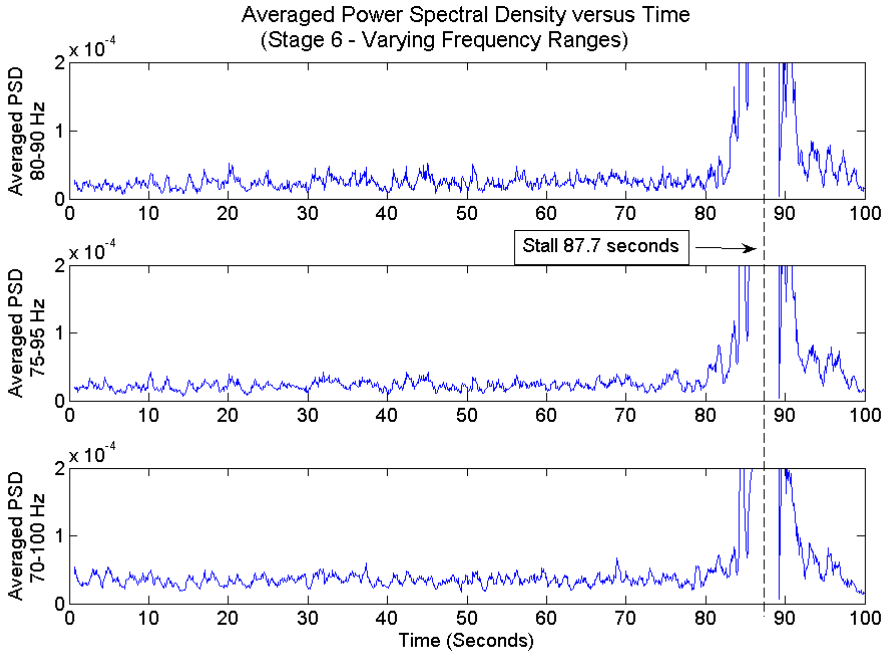

Figure 31. High-Speed Stall Stage 6 Power Spectral Density versus Time Varying Frequency Ranges

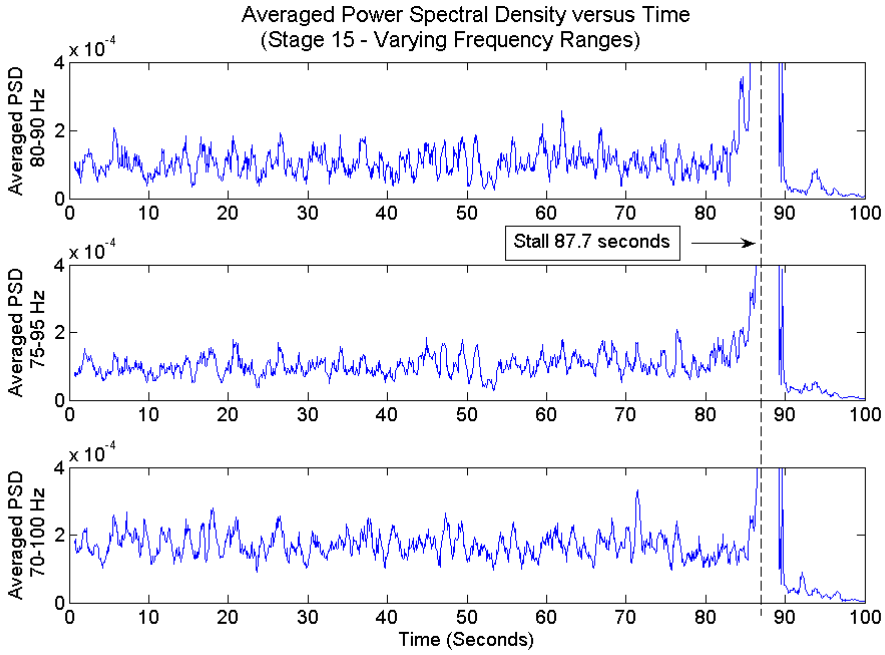

Figure 32. High-Speed Stall Stage 15 Power Spectral Density versus Time with Varying Frequency Ranges

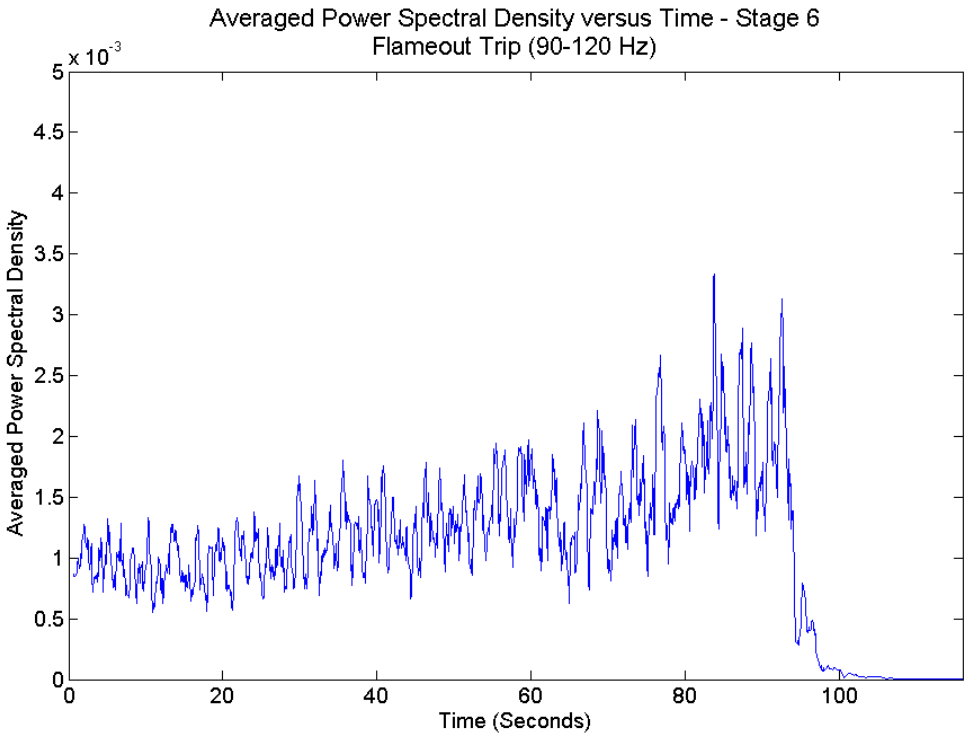

Figure 33. Flameout Trip Stage 6 Power Spectral Density versus Time

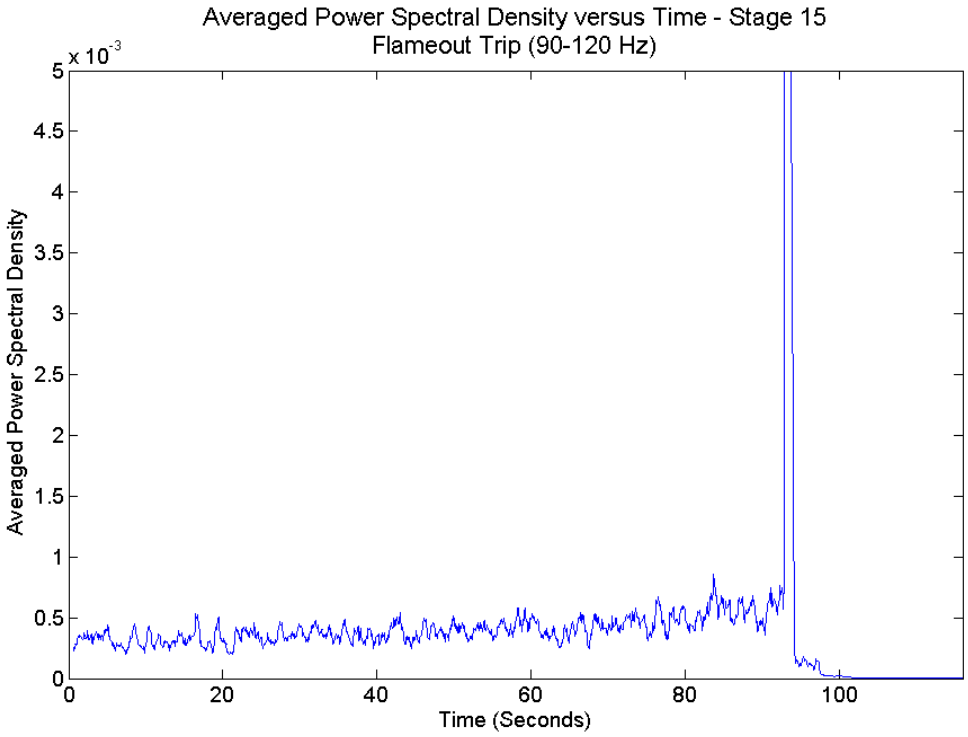

Figure 34. Flameout Trip Stage 15 Power Spectral Density versus Time

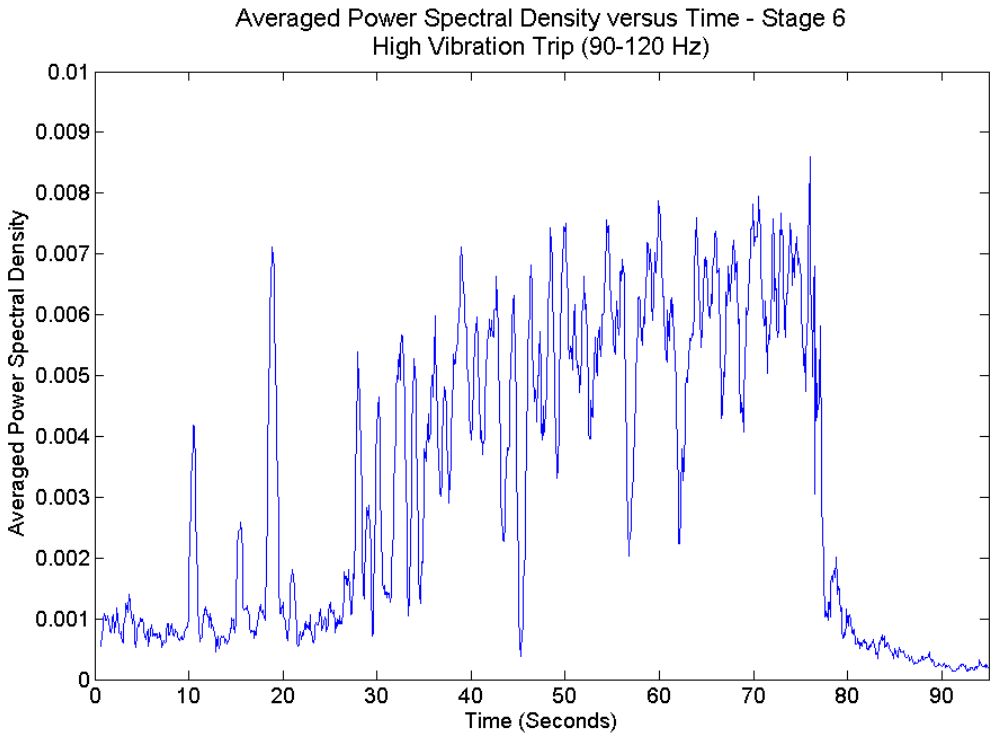

Figure 35. High Vibration Trip Stage 6 Power Spectral Density versus Time

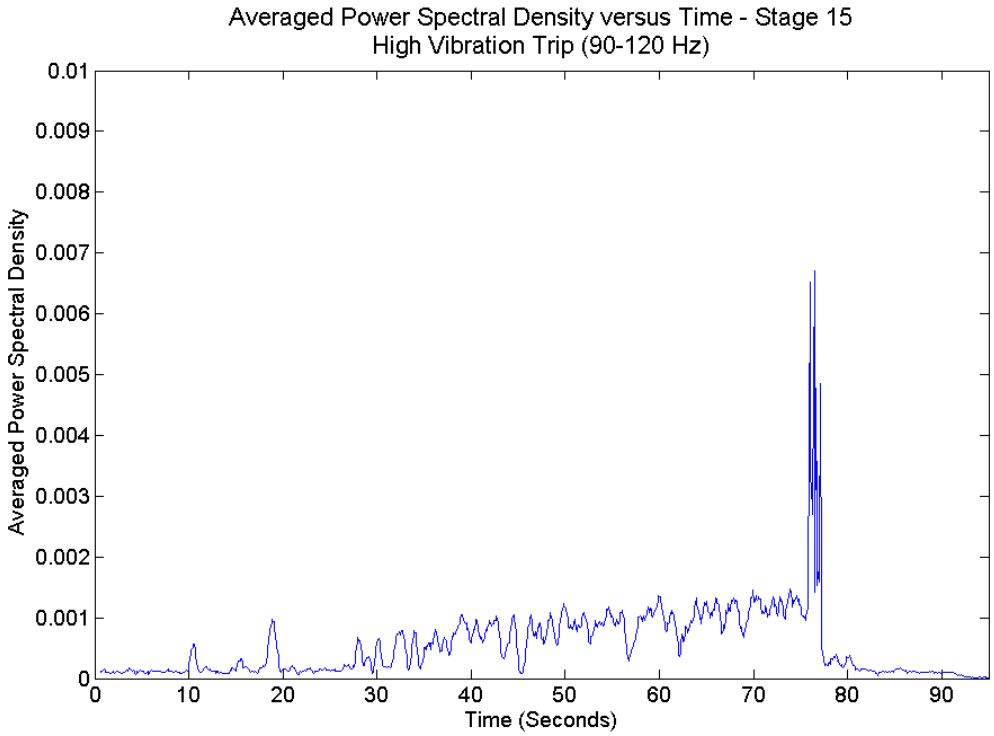

Figure 36. High Vibration Trip Stage 15 Power Spectral Density versus Time

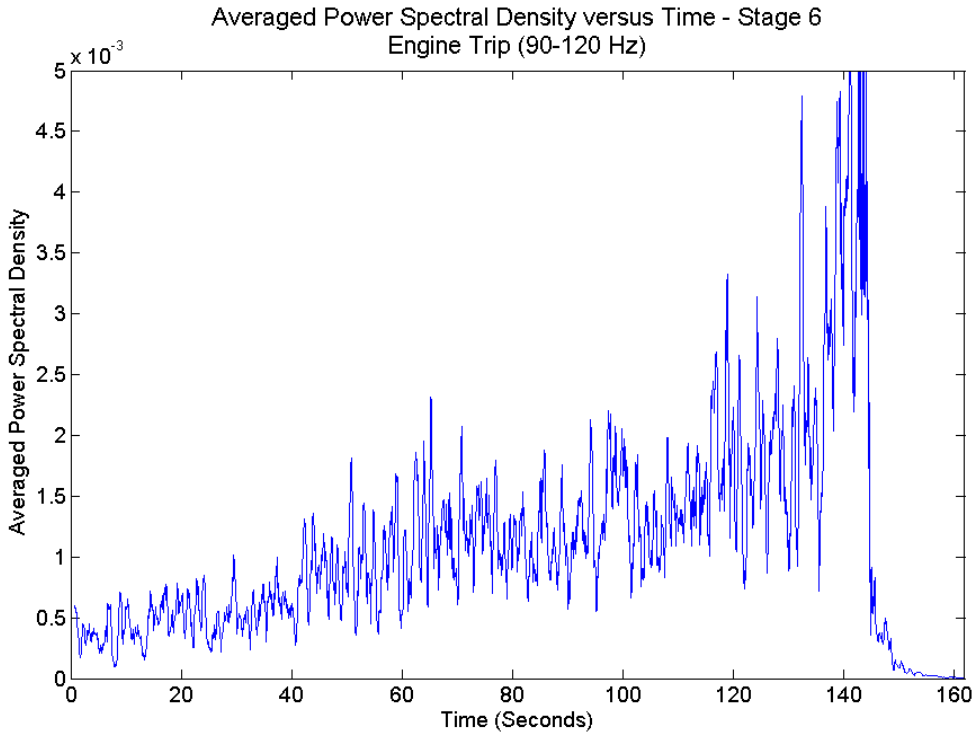

Figure 37. Engine Trip Stage 6 Power Spectral Density versus Time

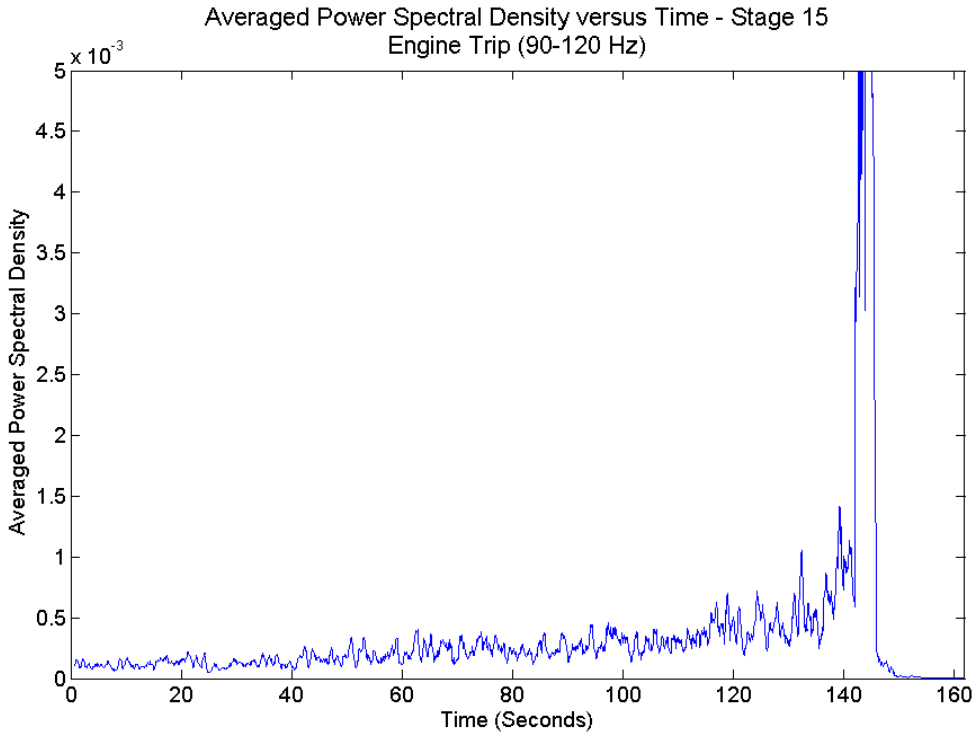

Figure 38. Engine Trip Stage 15 Power Spectral Density versus Time

C. AUTOCORRELATION FIGURES

The following figure is the averaged autocorrelation versus time for Stage 6 during the high-speed stall data run.

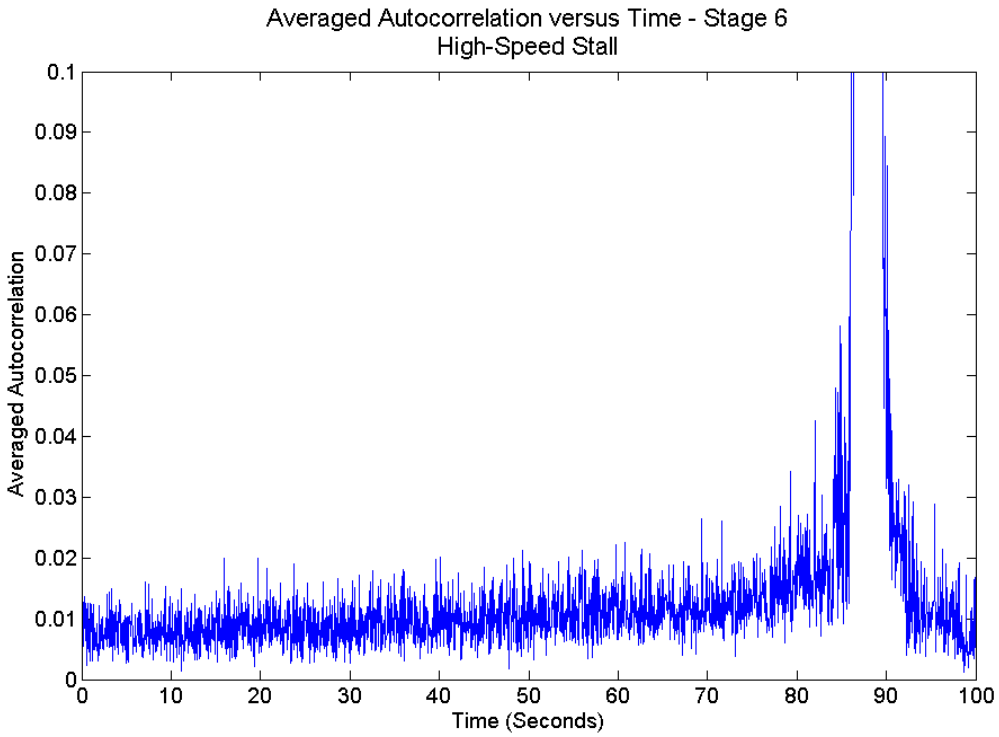

Figure 39. High-Speed Stall Stage 6 Autocorrelation versus Time

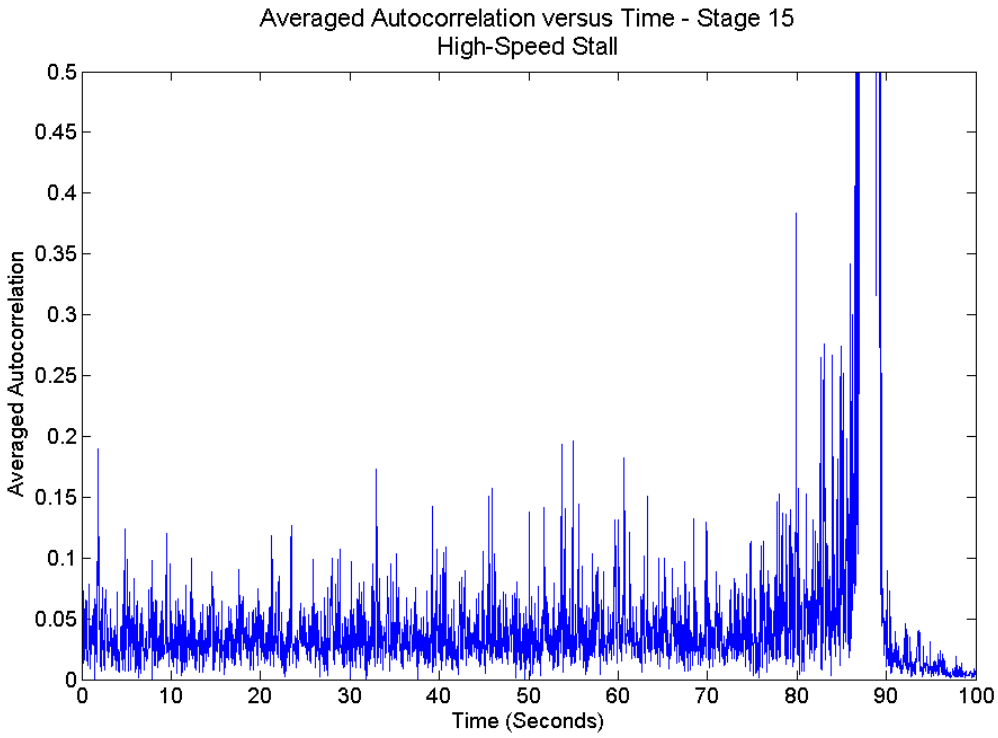

Figure 40. High Speed Stall Stage 15 Autocorrelation versus Time

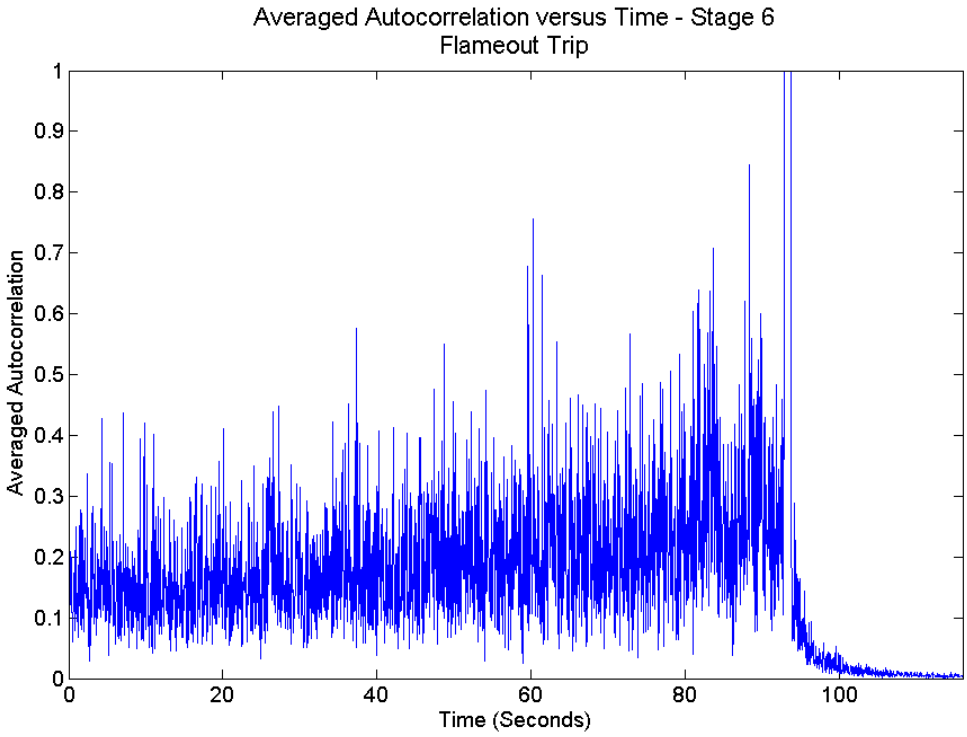

Figure 41. Flameout Trip Stage 6 Autocorrelation versus Time

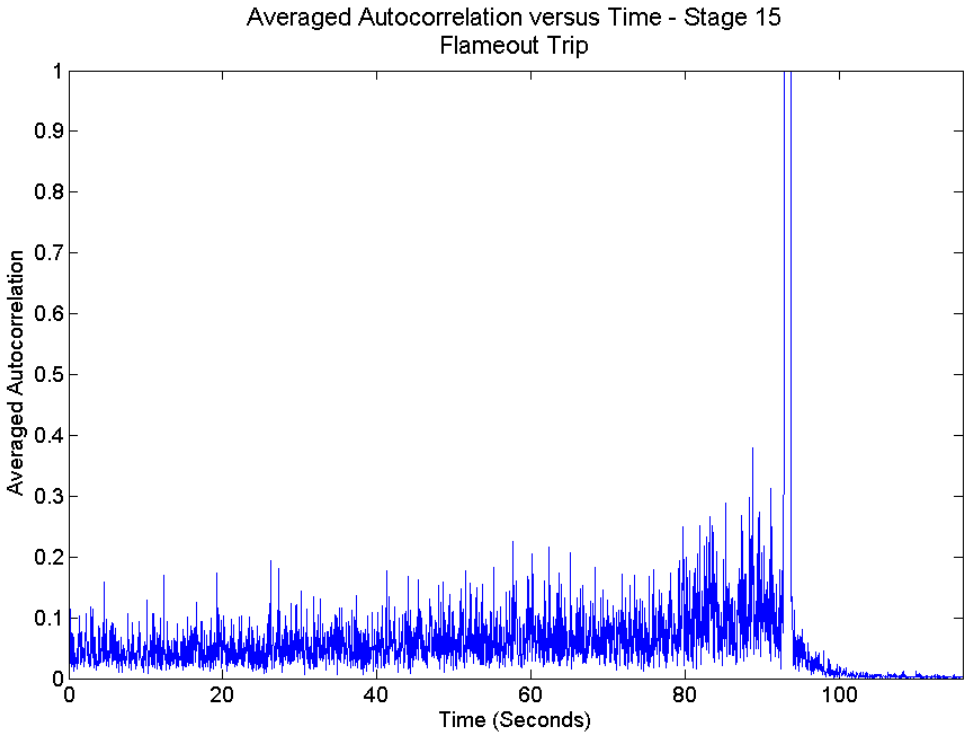

Figure 42. Flameout Trip Stage 15 Autocorrelation versus Time

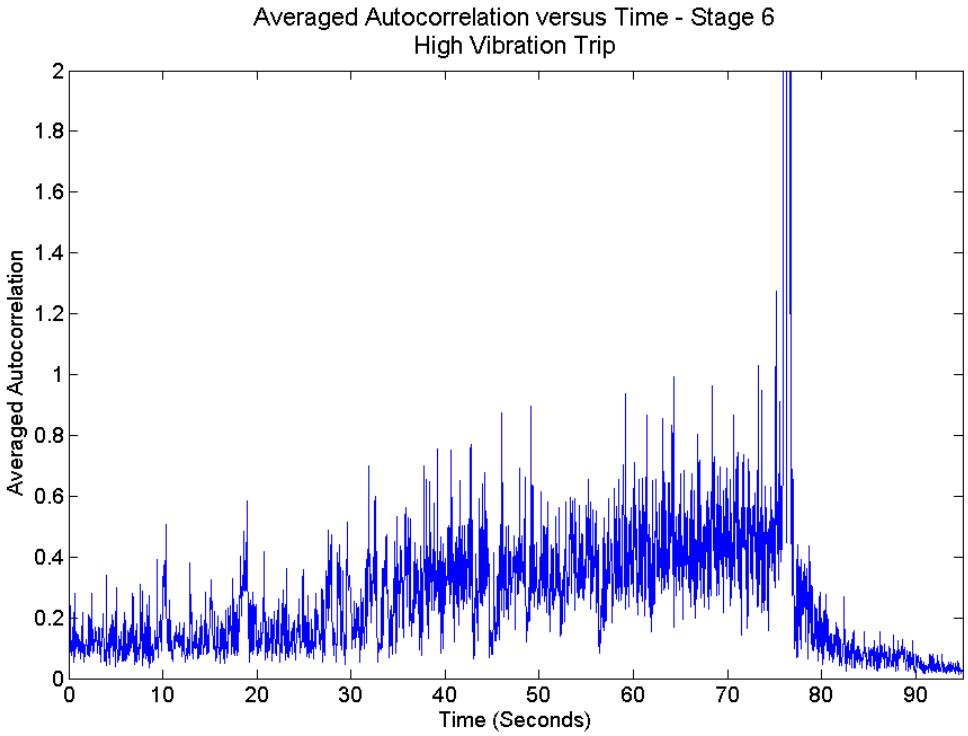

Figure 43. High Vibration Trip Stage 6 Autocorrelation versus Time

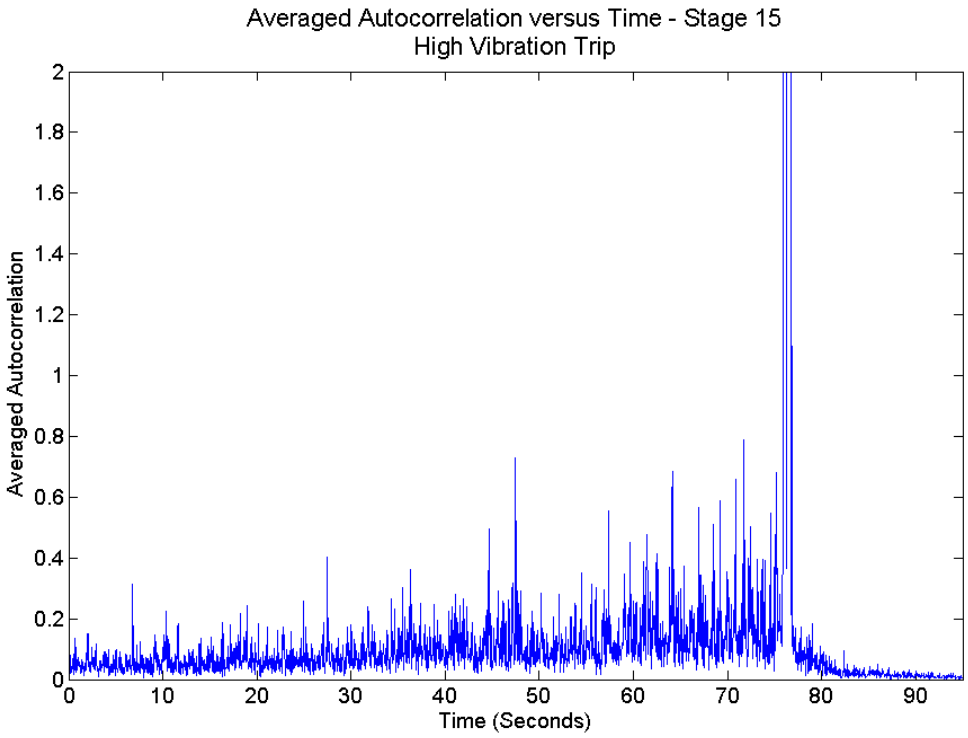

Figure 44. High Vibration Trip Stage 15 Autocorrelation versus Time

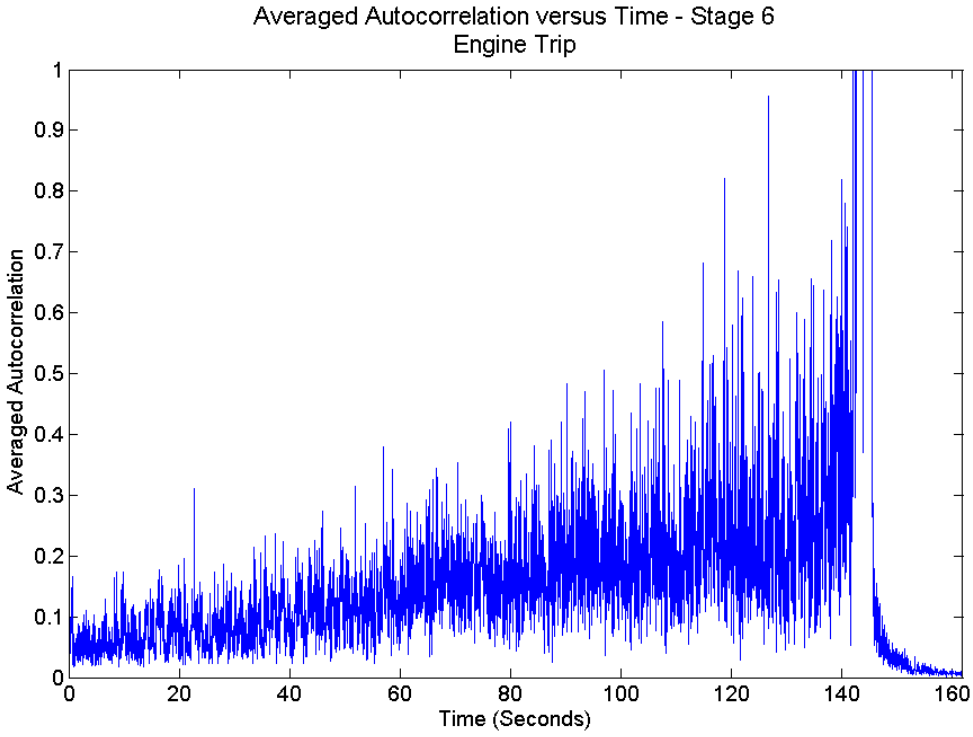

Figure 45. Engine Trip Stage 6 Autocorrelation versus Time

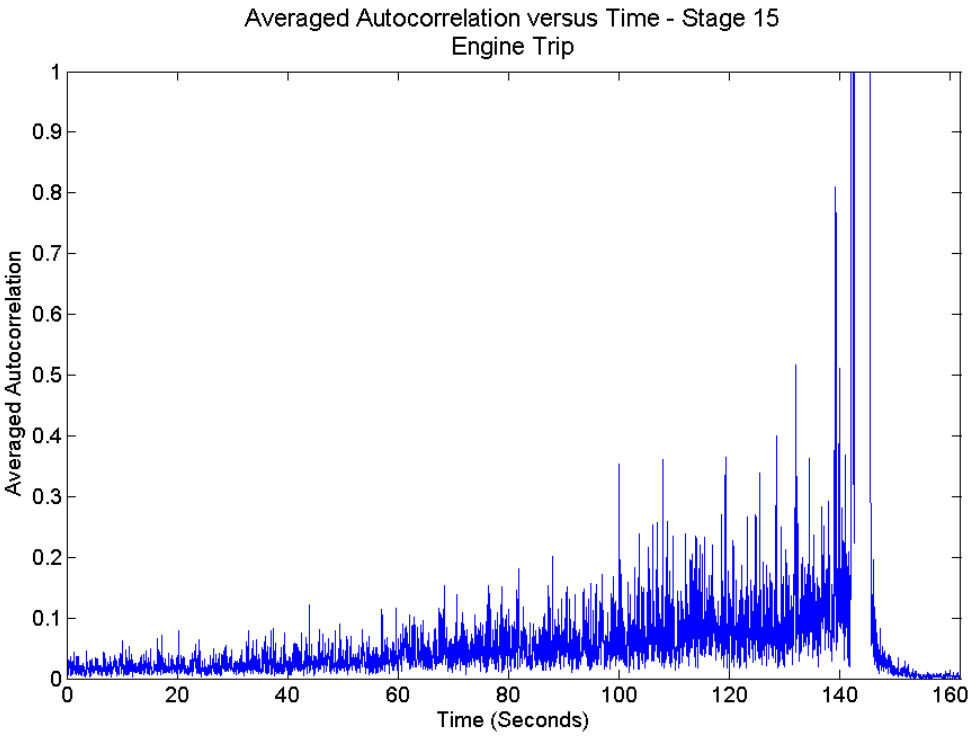

Figure 46. Engine Trip Stage 15 Autocorrelation versus Time

D. VARYING FFT VERSUS SAMPLING FREQUENCY

The following figure illustrates a constant FFT length of 2048 while varying the sampling frequency from 2048 to 12800 Hz.

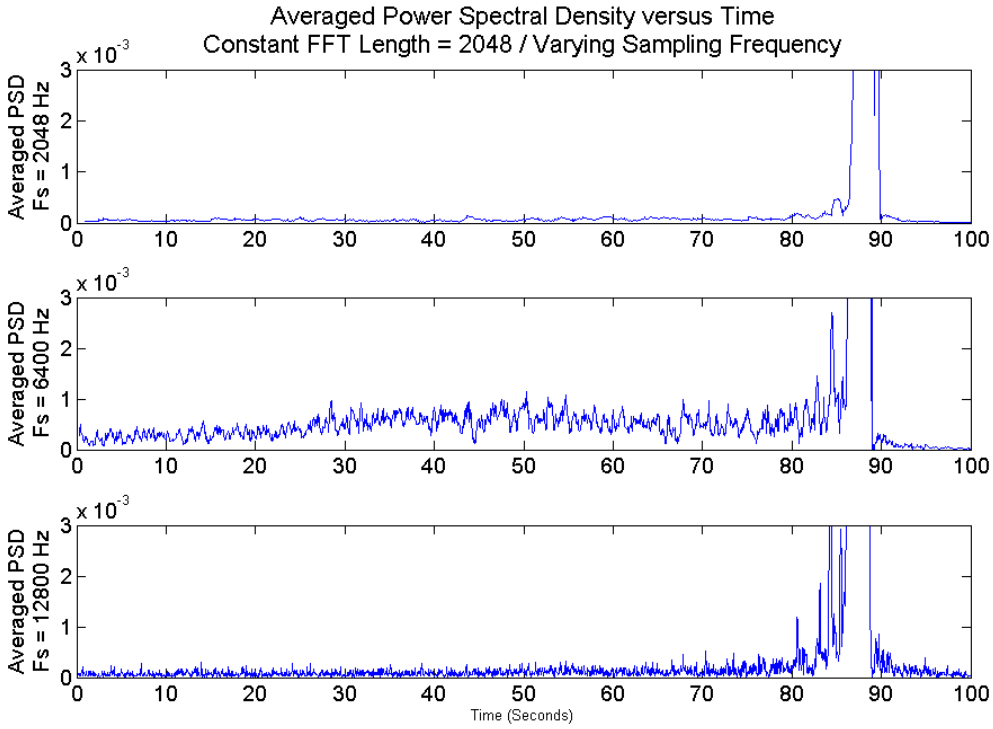

Figure 47. Average Power Spectral Density versus Time for a Constant FFT Length of 2048

The following figure illustrates a constant FFT length of 4096 while varying the sampling frequency from 2048 to 12800 Hz.

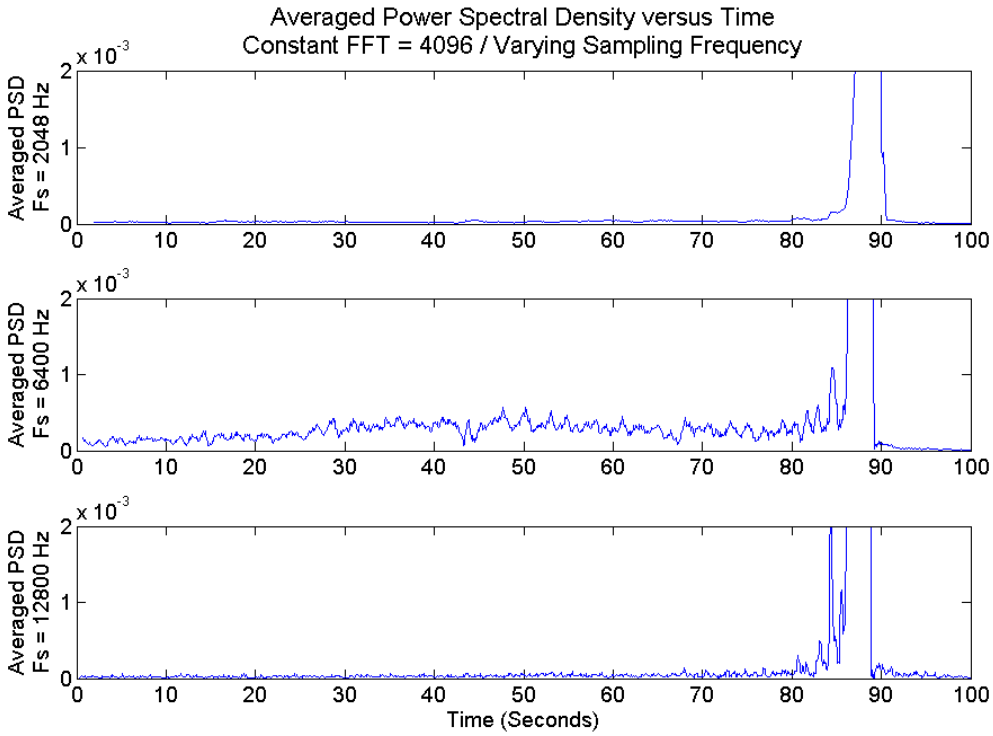

Figure 48. Average Power Spectral Density versus Time for a Constant FFT Length of 4096

The following figure illustrates a constant sampling frequency of 2048 Hz while varying the FFT length from 1024 to 4096.

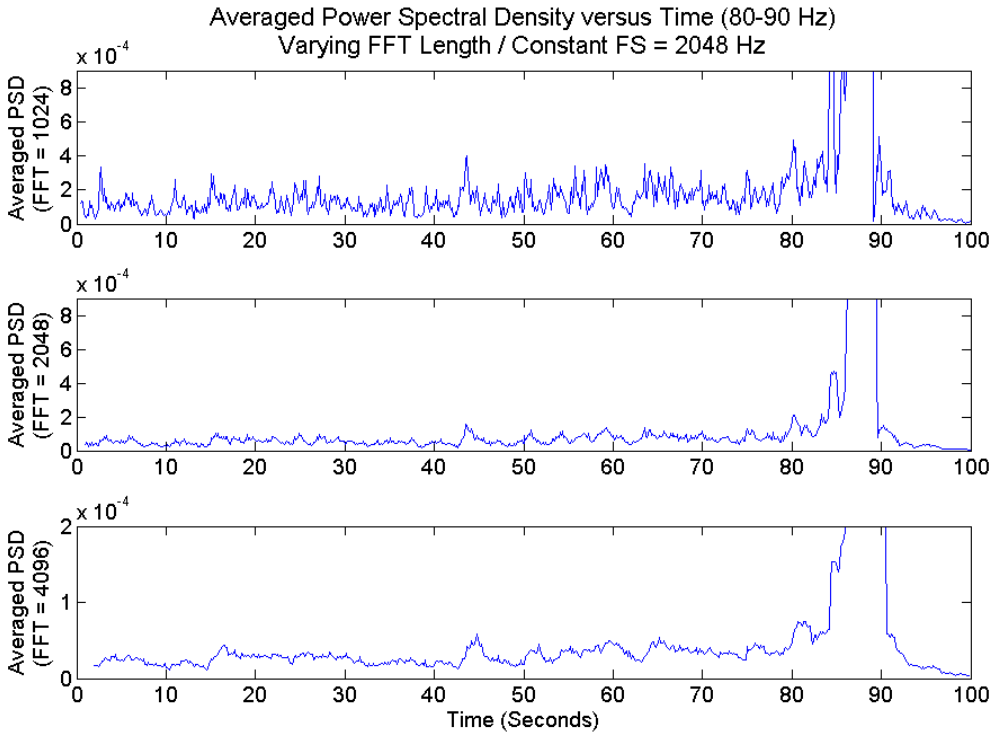

Figure 49. Average Power Spectral Density versus Time for a Constant Sampling Frequency of 2048 Hz.

The following figure illustrates a constant sampling frequency of 6400 Hz while varying the FFT length from 1024 to 4096.

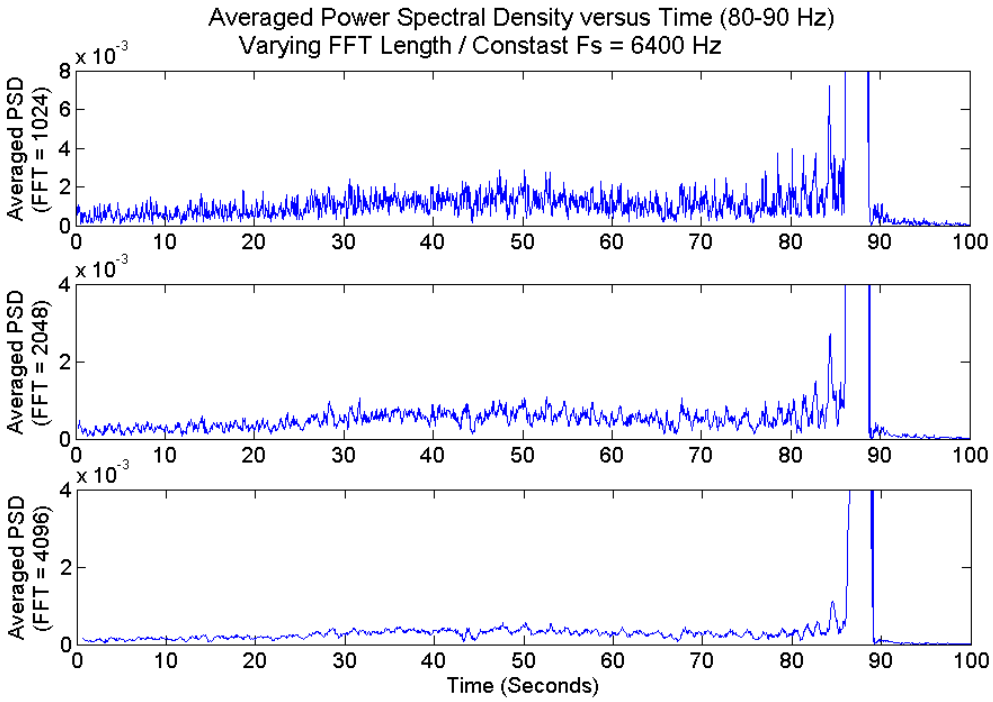

Figure 50. Average Power Spectral Density versus Time for a Constant Sampling Frequency of 6400 Hz.

THIS PAGE INTENTIONALLY LEFT BLANK

LIST OF REFERENCES

1. Emmons, H. W., Pearson, C. E., and Grant, H.P., “Compressor surge and stall propagation,” *Transactions of the ASME,* Volume Number 77, pp. 455-469, 1955.
2. Mcdougall, N. M., Cumpsty, N. A., and Hynes, T. P., “Stall Inception in Axial Compressors,” *Transactions of the ASME,* Volume Number 112, pp. 116-125, 1990.
3. Inoue, M., Kuroumaru, M. Iwamoto, T. and Ando, Y., “Detection of a Rotating Stall Precursor in Isolated Axial Flow Compressor Rotors,” *Journal of Turbomachinery,* Volume Number 113, pp. 281-289, 1991.
4. Day, I. J., “Stall Inception in Axial Flow Compressors,” *Journal of Turbomachinery,* Volume Number 115, pp. 1-9, 1993.
5. Tryfonidis, M., Etchevers, O., Paduano, J. D., Epstein, A. H., and Hendricks, G. J., “Prestall Behavior of Several High-Speed Compressors,” *Transactions of the ASME,* Volume Number 117, pp. 62-80, 1995.
6. Bright, M. M., Qammar, H. K., Weigl, H. J., and Paduano, J. D., “Stall Precursor Identification in High-Speed Compressor Stages Using Chaotic Time Series Analysis Methods,” *Journal of Turbomachinery,* Volume Number 119, pp. 491-500, 1997.
7. Camp, T. R., and Day, I. J., “A Study of Spike and Modal Stall Phenomena in a Low-Speed Axial Compressor,” *Journal of Turbomachinery,* Volume Number 120, pp. 393-401, 1998.
8. Hoying, D. A., “Stall Inception in a Multistage High-Speed Axial Compressor,” *Journal of Propulsion and Power,* Volume Number 11, pp. 915-922, 1995.
9. Day, I. J., Breuer, T., Escuret, J., Cherrett, M., and Wilson, A., “Stall Inception and the Prospects for Active Control in Four High-Speed Compressors,” *Transactions of the ASME,* Volume Number 121, pp. 18-27, 1999.
10. Bright, M. M., Qammar, H. K., and Wang, L., Ínvestigation of Pre-stall Mode and Pip Inception in High-Speed Compressors Through the Use of Correlation Integral,” *Journal of Turbomachinery,* Volume Number 121, pp. 743-750, 1999.
11. Hoss, B., Leinhos, D., and Fottner, L., “Stall Inception in the Compressor System of a Turbofan Engine,” *Transactions of the ASME,* Volume Number 122, pp. 32-44, 2000.
12. Cadzow, J. A., (1987). *Foundations of Digital Signal Processing and Data Analysis.* New York, NY: Macmillan Publishing Company.

13. Cooley, J. W., and Tukey, J. W., "An Algorithm for the Machine Computation of the Complex Fourier Series," *Mathematics of Computation,* Volume Number 19, pp. 297-301, 1965.

INITIAL DISTRIBUTION LIST

1. Defense Technical Information Center
   Ft. Belvoir, Virginia

2. Dudley Knox Library
   Naval Postgraduate School
   Monterey, California

3. Professor Knox T. Millsaps
   Department of Mechanical and Astronautical Engineering
   Naval Postgraduate School
   Monterey, California

4. Professor Garth V. Hobson
   Department of Mechanical and Astronautical Engineering
   Naval Postgraduate School
   Monterey, California

5. Distinguished Professor Anthony J. Healey
   Department of Mechanical and Astronautical Engineering
   Naval Postgraduate School
   Monterey, California

6. Mr. Jeffrey Patterson
   Head of Gas Turbine Emerging Technologies Section – Code 9334
   NAVSEA, NSWC Philadelphia
   Philadelphia, Pennsylvania

7. Mr. John Scharschan
   Gas Turbines – Emerging Technologies – Code 9334
   NAVSEA, NSWC Philadelphia
   Philadelphia, Pennsylvania

8. Daniel E. Caguiat
   Code 9334
   NAVSEA, NSWC Philadelphia
   Philadelphia, Pennsylvania